MATHEMATICAL MODELING
OF CLOUD CHEMISTRY
IN THE CALIFORNIA SOUTH COAST AIR BASIN

Contract Number A732-042

December 1988

Prepared for

California Air Resources Board
1800 15th Street
Sacramento, CA 95814

Prepared by

Christian Seigneur
Anthony M. Wegrecki
Bechtel Environmental, Inc.
50 Beale Street
P.O. Box 3965
San Francisco, CA 94119

and

L. Willard Richards
Sonoma Technology, Inc.
5510 Skylane Boulevard, Suite 101
Santa Rosa, CA 95403

ACKNOWLEDGMENTS

The authors gratefully acknowledge the continuous support of the Project Officers, Mr. Eric M. Fugita, Dr. Praveen K. Amar and Mr. Bart Croes of the California Air Resource Board. Thanks are also due to Mr. Vince A. Mirabella of the Southern California Edison Company for allowing us to use the PLMSTAR air quality model for this study.

This report was submitted in fulfillment of Contract No. A732-042, Modeling of Cloudwater Chemistry in the South Coast Air Basin by Bechtel Environmental, Inc. and Sonoma Technology, Inc. under the sponsorship of the California Air Resources Board. Work was completed as of June 1988.

ABSTRACT

A mathematical model of cloud chemistry was evaluated with the cloud chemistry data collected by Richards et al. from 1981 to 1985 in stratus clouds in the Los Angeles basin. The model simulates atmospheric chemistry including gas-phase chemistry, aqueous-phase chemistry and gas/droplet mass transfer, vertical transport, rainfall and turbulent diffusion.

Evaluation of the model entailed evaluation of the equilibrium chemistry, chemical kinetics and transport processes. The equilibrium chemistry was evaluated with a total of 52 case studies. Comparison of measured and predicted hydrogen ion concentrations showed, on average, an underprediction of 3% and an absolute error of 20%. The equilibrium chemistry of sulfur (IV) suggests that there was sulfur (IV) present as hydroxymethane sulfonic acid. There was good agreement between measured and calculated gas/liquid distributions of formaldehyde. However, there was a large discrepancy between the measured and calculated gas/liquid distributions of acetaldehyde suggesting that the aqueous-phase acetaldehyde concentrations are underestimated by about a factor of 40. The chemical kinetics was evaluated with five case studies for which cloud chemistry data were collected in the same air parcel at different times, covering periods of up to 3 hours. The results showed that the model underestimated nitrate formation in three cases and gave good agreement with the data in two cases. Concentrations of sulfur dioxide were too low to allow evaluation of the model for sulfate. These results suggested that vertical transport was a major process governing the chemical composition of stratus clouds and needs to be included in a cloud chemistry model.

The model with treatment of cloud chemistry, vertical transport and diffusion was evaluated with two case studies. For one case study, which corresponded to an air parcel moving from offshore toward Los Angeles, there were discrepancies between measured and calculated concentrations of major species. This result suggests that transport processes may be more complex than the one-dimensional transport simulated by the model. For the other case study, which corresponded to an air parcel moving over the eastern Los Angeles basin, there was very good agreement between measured and calculated concentrations of major species. This result suggests that the chemistry, updraft and rainfall were reasonably well simulated with the model.

A total of 19 sensitivity analysis simulations was performed with this latter case study. The sensitivity of sulfate, nitrate, ammonium and hydrogen ion concentrations to percursor levels, various chemical kinetic and cloud microphysical parameters and various environmental conditions were discussed.

A mechanism for the chemistry of organic acids was developed and applied to this case study.

"The statements and conclusions in this report are those of the contractor and not necessarily those of the California Air Resources Board. The mention of commercial products, their source or their use in connection with material reported herein is not to be construed as either an actual or implied endorsement of such products."

TABLE OF CONTENTS

	Page
Summary and Conclusions	1-1
Recommendations	2-1
Introduction	3-1
Experimental Data	4-1
Description of the Cloud Model	5-1
Equilibrium Chemistry	6-1
Chemical Kinetics	7-1
Chemical Kinetics and Transport	8-1
Sensitivity Analysis Studies	9-1
Cloud Chemistry of Organic Acids	10-1
References	11-1

LIST OF TABLES

		Page
Table 4-1.	Input Data for the Cloud Model	4-5
Table 5-1.	The Carbon-Bond Mechanism IV	5-4
Table 5-2.	Equilibrium Reactions with Temperature Dependence	5-9
Table 5-3.	Aqueous Phase Kinetics	5-11
Table 6-1.	Comparison of Calculated and Measured pH Values at Equilibrium	6-3
Table 6-2.	Normalized Bias and Absolute Error in H^+ Concentrations	6-5
Table 6-3.	Comparison of Measured and Calculated S(IV) Concentrations	6-8
Table 6-4.	Comparison of Measured and Calculated Aldehyde Concentrations	6-10
Table 7-1.	Comparison of Measured and Calculated Solute Concentrations. Case Study of 21 May 1985	7-3
Table 7-2.	Comparison of Measured and Calculated Gas Concentrations. Case Study of 21 May 1985	7-4
Table 7-3.	Comparison of Measured and Calculated Solute Concentrations. Case Study of 25 May 1985	7-7
Table 7-4.	Comparison of Measured and Calculated Gas Concentrations. Case Study of 25 May 1985	7-8
Table 7-5.	Comparison of Measured and Calculated Solute Concentrations. Case Study of 26 May 1985	7-10
Table 7-6.	Comparison of Measured and Calculated Gas Concentrations. Case Study of 26 May 1985	7-11
Table 7-7.	Comparison of Measured and Calculated Solute Concentrations. Case Study of 27 May 1985	7-12

LIST OF TABLES

		Page
Table 7-8.	Comparison of Measured and Calculated Gas Concentrations. Case Study of 27 May 1985	7-14
Table 7-9.	Comparison of Measured and Calculated Solute Concentrations. Case Study of 10 June 1985	7-15
Table 7-10.	Comparison of Measured and Calculated Gas Concentrations. Case Study of 10 June 1985	7-17
Table 7-11.	Comparison of Measured and Calculated Nitrate Formation	7-19
Table 7-12.	Contribution of Major Chemical Pathways to Nitrate Formation	7-20
Table 7-13.	Comparison of Measured and Calculated Sulfate Formation	7-22
Table 7-14.	Contribution of Major Chemical Pathways to Sulfate Formation	7-24
Table 8-1.	Initial Concentrations of Major Chemical Species below and in the Cloud - Simulation of 25 May 1985	8-4
Table 8-2.	Initial Concentrations of Major Chemical Species below and in the Cloud - Simulation of 26 May 1985	8-5
Table 8-3.	Comparison of Measured and Calculated Cloud Concentrations of Major Chemical Species - Simulation of 25 May 1985	8-7
Table 8-4.	Comparison of Measured and Calculated Cloud Concentrations of Major Chemical Species - Simulation of 26 May 1985	8-10

LIST OF TABLES

		Page
Table 9-1.	Sensitivity Studies Performed with the Simulation of 26 May 1985	9-2
Table 9-2.	Major Species Concentrations after Two Hours for Various Precursor Levels	9-5
Table 9-3.	Nitrate and Hydrogen Ion Concentrations after Two Hours for Various Nitrate Formation Kinetics	9-8
Table 9-4.	Major Species Concentrations after Two Hours for Various Values of Cloud Physics Parameters	9-10
Table 9-5.	Major Species Concentrations after Two Hours for Various Environmental Conditions	9-13
Table 10-1.	Chemical Kinetic Mechanism for Organic Acids	10-2

LIST OF FIGURES

		Page
Figure 5-1.	Schematic Representation of the Cloud Model	5-2
Figure 5-2.	Schematic Description of the Cloud Microphysical Processes	5-15
Figure 9-1.	Sulfate Cloud Concentrations and Wet Deposition after Two Hours as Function of the Initial SO_2 Concentration	9-4

Section 1

SUMMARY AND CONCLUSIONS

SUMMARY

A mathematical model of cloud physics and chemistry was evaluated with the cloud chemistry data collected in stratus clouds in the California SoCAB from 1981 to 1985 by Richards et al. (1983a, 1985, 1987). This mathematical model simulates transport, diffusion and rainfall as well as atmospheric chemistry. The treatment of chemistry includes gas-phase chemistry, gas/droplet mass transfer and aqueous-phase chemistry.

EQUILIBRIUM CHEMISTRY

First, the equilibrium chemistry of the model was evaluated. A total of 52 case studies was used to assess model performance. The average normalized bias and absolute error in the hydrogen ion (H^+) concentration are -3 percent and 20 percent, respectively. If it is assumed that hydroxymethane sulfonic acid (HMSA), a species resulting from the reaction of sulfur dioxide with formaldehyde in solution, was present in cloud droplet, the bias becomes 0.2 percent and the absolute error remains 20 percent. The most recent data set, which was collected in 1985, shows a clear trend toward underpredictions of H^+.

Analysis of the chemistry of sulfur in oxidation state IV (S(IV)) shows that the aqueous concentrations of S(IV) that were measured can only be explained if HMSA was present.

Comparison of measured and calculated formaldehyde and acetaldehyde concentrations shows that the equilibrium chemistry of formaldehyde is simulated correctly but that a large discrepancy exists between

the calculated and measured gas/liquid distributions of acetaldehyde. The calculated aqueous concentration of formaldehyde is, on average, about 60 percent higher than the measured concentration. The calculated aqueous concentration of acetaldehyde is on average about 40 times smaller than the measured concentration.

CHEMICAL KINETICS

The data collected in 1985 by Richards et al. (1987) provide information on the evolution of cloud chemistry with time. Five case studies were used to evaluate the treatment of chemical kinetics by the model. Comparison of measured and calculated values of chemical species concentrations can not be explained solely by chemical kinetics. This result suggests that upward transport of pollutants from below the cloud into the cloud was an important process. In three cases (simulations of 21, 25 and 26 May 1985), nitrate concentrations are underestimated by the model, probably because transport was not simulated. In the two other cases (simulations of 27 May and 10 June 1985), the measured and calculated initial concentrations are in good agreement. The two major pathways leading to nitrate formation are the heterogeneous hydrolysis of nitrogen pentoxide (N_2O_5) and the aqueous reduction of nitrate (NO_3) radicals.

Because the sulfur dioxide (SO_2) concentrations were below 1 part per billion (ppb), which is the measurement uncertainty, it is not feasible to evaluate model performance for sulfate formation. The major pathway for sulfate formation is the aqueous oxidation of SO_2 by hydrogen peroxide (H_2O_2). The aqueous catalyzed oxidation of SO_2 by oxygen (O_2) and the aqueous oxidation of SO_2 by hydroxyl (OH) radicals also contribute noticeably to sulfate formation.

Two cases were selected to analyze the cloud chemistry and vertical transport processes: 25 May and 26 May 1985. These two case studies were selected because they show significant increases in

nitrate concentrations. A cloud microphysics model was used to estimate the updraft velocities which were not otherwise available. Below-cloud concentrations of several species were not available and were estimated from 24-hour average data and other data on typical values and diurnal variations of these species in the SoCAB.

The simulation of 25 May 1985 does not predict correctly the measured cloud species concentrations, which suggests that NO_x emissions from tall stacks may contribute significantly to NO_x concentrations in coastal clouds, and that the below-cloud concentrations of sulfate and nitrate may not have been estimated accurately.

The simulation of 26 May 1988 shows very good agreement between calculated and measured values. There was some light drizzle observed on that day and the good agreement between the calculated and measured concentrations of inert species suggests that the model simulates well the updraft and rainfall processes. Calculated and measured concentrations of sulfate and nitrate and acidity (pH) are in good agreement. It seems that the model treats satisfactorily the major physical and chemical processes for this case study.

SENSITIVITY ANALYSES

Several sensitivity analyses were conducted with this latter simulation. Variations of precursor levels show that the SO_2/sulfate relationship is nonlinear and that the nitrogen oxides (NO_x)/nitrate relationship is nearly linear. (A relationship is linear if a given fractional change in the precursor level leads to the same fractional change in the pollutant; otherwise, this relationship is nonlinear). A reduction in RHC concentrations has little effect on cloud chemistry whereas a reduction in NH_3 concentrations leads to a direct increase in pH. It should be noted, however, that changes in NO_x and RHC concentrations may

lead to nonlinear changes in sulfate and nitrate concentrations on longer time scales due to the effect of these species on oxidant concentrations.

The effect of N_2O_5 and NO_3 kinetics on nitrate formation was investigated. The use of a rate of N_2O_5 hydrolysis limited only by diffusion leads to an increase in nitrate formation of 30%. The aqueous chemistry of NO_3 shows little sensitivity to the accommodation coefficient, except at very low values of this coefficient.

The effect of the updraft velocity and cloud water content on cloud chemistry was investigated. The contribution of species initially below the cloud to the cloud chemical composition increases as the updraft velocity increases. For the case considered, the contribution of species initially below the cloud leads to a higher pH in cloud droplets. The increase in cloud water content leads to an increase in sulfate formation because more liquid water volume is available for reactions such as the aqueous oxidation of SO_2 by O_2 and OH. There is only a slight increase in nitrate formation because the increase in the NO_3 aqueous reduction pathway is compensated by a decrease in the N_2O_5 hydrolysis pathway.

The effect of the environmental conditions on acid formation was investigated. A daytime simulation shows a slight increase in sulfate formation due to an increase in the aqueous reaction of SO_2 with OH. The nitrate formation pathway changes significantly as reaction of nitrogen dioxide (NO_2) with OH predominates and the NO_3 and N_2O_5 pathways become minor.

The simulation of a nonraining cloud shows a lower pH as the acid species concentrations are higher since no removal of sulfate or nitrate by rain takes place.

The simulation of a cloud-free nighttime scenario shows that no sulfate formation takes place since no aqueous medium is available for SO_2 oxidation. Nitrate formation takes place to a small extent through N_2O_5 hydrolysis.

In a fog simulation, sulfate formation takes place primarily through aqueous oxidation of SO_2 by O_2 and H_2O_2. Formation of nitrate occurs through oxidation of NO_2 by OH; NO_3 concentration are low because of the high NO and low O_3 concentrations.

Simulation of a plume in a cloud suggests that HMSA can be formed rapidly as SO_2 reacts with HCHO in cloud droplets. The slow rate of the HMSA decomposition explains the presence of HMSA in SoCAB stratus clouds.

A chemical kinetic mechanism was developed for major organic acids, i.e, formic, acetic and peroxyacetic acids. Simulation of the 26 May 1985 scenario shows little organic acid formation because the chemistry of organic acid formation is primarily driven by OH and HO_2 radicals, which are present in very small concentrations for this nighttime scenario. Daytime chemistry of organic acids should be investigated.

Section 2
RECOMMENDATIONS

Based on the results of this study, the following recommendations can be made.

1. Future cloud chemistry measurement programs should include measurements below the cloud in addition to the in-cloud measurements because vertical transport is a major process governing cloud chemical composition, even in stratiform clouds.

2. Tracer experiments would be extremely useful to help understand transport phenomena occurring in clouds. These transport phenomena may be more complicated than a simple one-dimensional updraft, even for stratiform clouds.

3. Organic acid measurements in clouds and fogs would be useful to assess the contribution of organic acids to cloud acidity.

4. The gas/liquid equilibrium of acetaldehyde needs to be studied in the laboratory, since theoretical calculations and measurements are in disagreement by about a factor of 40.

5. The effect of precusor concentrations (particularly, NO_x and RHC) on acid concentrations should be studied by means of three-dimensional one-day or multi-day simulations, because of the effect of these precursors on the daytime chemistry of oxidant formation.

6. Organic acid formation should be simulated for daytime conditions to assess its importance; results should be compared to available measurements.

7. The heterogeneous hydrolysis of N_2O_5 needs to be studied in more detail since it is a major pathway for nocturnal formation of nitrate.

REGULATORY IMPLICATIONS

The results of this modeling study demonstrate that the mathematical model of atmospheric chemistry and physics used in this study can describe satisfactorily the major chemical and physical processes that lead to acid formation. For the cases where model performance is satisfactory, the model can be applied to evaluate the effect of emission control strategies. It should be noted, however, that larger temporal (e.g., of the order of one day) and spatial (e.g., basinwide) scales should be used when developing emission control strategies.

Section 3
INTRODUCTION

The formation of sulfate and nitrate species in the California South Coast Air Basin (SoCAB) is a topic of great importance in air quality because these species lead to acid deposition, visibility degradation, and increased aerosol concentrations.

The California Air Resources Board (CARB) has sponsored several field programs over the past four years to characterize the reactants, products, kinetics and mechanisms of stratus cloud chemistry in the SoCAB (Richards et al., 1983a, 1985, 1987). The experimental results obtained during these field programs are very comprehensive and constitute a unique data base for a detailed investigation of the chemistry of stratus clouds in the SoCAB. Some topics of particular interest for our understanding of cloud chemistry in the SoCAB include the following.

1. Evaluation of the equilibrium chemistry and kinetics of sulfate and nitrate formation in clouds.
2. Identification of the most important chemical pathways leading to sulfate and nitrate formation.
3. Investigation of the relationships between precursors and acid species concentrations.
4. Analysis of the sensitivity of cloud chemistry to various meteorological and chemical parameters.

These topics have been addressed to some extent by Seigneur and Saxena (1984) and Seigneur et al. (1985) using the data of Richards et al. (1983a) as input to a detailed chemical kinetic mechanism of cloud chemistry. However, the data of Richards et al. (1985, 1987) provide a more complete data base which can be used to perform a more comprehensive evaluation of a cloud chemistry model. In particular, the data of Richards et al. (1987) provide unique

information regarding the evolution of an air parcel in a stratus cloud for time periods of up to 3 hours. These data also include measurements of both gas and aqueous-phase concentrations of formaldehyde and acetaldehyde.

In this study, a comprehensive computerized mathematical model of cloud chemistry and physics was used to investigate the chemical and physical processes that govern the formation of acidic species in clouds. First, the performance of the model treatment of equilibrium chemistry and chemical kinetics is evaluated. Then, the model was used to investigate the chemical pathways and transport processes that lead to acid formation in clouds and to study the sensitivity of the acid concentrations to various chemical and meteorological parameters.

Section 4 presents a brief overview of the experiemental data used for this study. Section 5 presents a description of the cloud model. Sections 6 and 7 present the results of the model performance evaluation for equilibrium chemistry and chemical kinetics, respectively. Section 8 presents the results of model performance evaluation when both chemical kinetics and atmospheric transport are considered. The chemistry and physics of acid formation in clouds is investigated in detail through sensitivity analyses for one case study in Section 9. The cloud chemistry of organic acids is addressed in Section 10.

Section 4
EXPERIMENTAL DATA

OVERVIEW OF THE EXPERIMENTAL DATA

The data collected by Richards et al. (1983a, 1985, 1987) provide the basis for this study. Therefore, it is worthwhile to present a brief overview of the major results deduced from these data.

- The measured pH of cloudwater varied between 2.3 and 4.7, and was about 3 on average.

- The cloud water composition is about 40 to 50% nitric acid (HNO_3), 20 to 30% ammonium sulfate ($(NH_4)_2SO_4$) and 10 to 20% sodium chloride (NaCl). Note that this composition is given for convenience and does not imply that for instance, the ammonium is associated solely with sulfate and the hydrogen solely with nitrate.

- The agreement between the measured value of pH and the value calculated from an ionic balance was generally very good, particularly for the 1985 data (the ionic balance is correct within about 2 percent on average for the 1985 data). Similarly, good agreement was obtained between measured and calculated values of conductivity.

- Concentrations of sulfate and nitrate are rather uniform spatially. Exceptions correspond to measurements during the 1981-1982 program near Fontana in the vicinity of a large emission source of sulfur dioxide (SO_2) and nitrogen oxides (NO_x).

- In the 1981-1982 field program, significant concentrations of dissolved SO_2 (S(IV)(aq)) and hydrogen peroxide (H_2O_2 (aq)) were measured in the same cloud water samples. Because the aqueous oxidation of SO_2 by H_2O_2 is rapid, this result suggested the presence of S(IV)(aq) in complexed form that would inhibit its oxidation. Richards et al. (1983b) suggested that the formation of hydroxymethane sulfonic acid (HMSA) could account for some of this inhibition. However, computer simulations of these cases that were conducted by Seigneur and Saxena (1984) could not totally explain the presence of S(IV) and H_2O_2 in solution by the formation of HMSA.

It cannot be ruled out that the S(IV) aqueous concentration measurements had a bias toward overestimation. Clearly, this issue requires further investigation in this proposed study (the cloud chemistry model now treats the HMSA complex formation with two kinetic steps rather than with an equilibrium; this new treatment could lead to higher HMSA concentrations). In the two subsequent programs, no significant amount of SO_2 was measured in clouds. There was enough H_2O_2 present to oxidize from 0.2 to 4 ppb of SO_2.

- The gas/liquid equilibrium chemistry of formaldehyde is in reasonable agreement with theory. However, the gas/liquid equilibrium chemistry of acetaldehyde appears to be off by a factor of 100 with theory; this discrepancy suggests that the present value of the Henry's law constant for acetaldehyde needs to be reevaluated.

- Ozone (O_3) concentrations in clouds were generally significantly less than O_3 concentrations outside of clouds. No evident explanation appears at the moment for this variation. Seigneur and Saxena (1985) showed by means of computer simulations of cloud chemistry that O_3 formation is less in clouds than in dry atmospheres, however, the predicted variation does not totally explain the variations observed by Richards et al. and further investigation is warranted.

- Concentrations of sodium (Na^+), potassium (K^+), calcium (Ca^{2+}), magnesium (Mg^{2+}), iron (Fe^{3+}) and manganese (Mn^{2+}) ions appear to decrease in clouds during the 1985 program. It was suggested that removal processes such as drizzling and vertical transport could account for this decrease.

- Concentrations of ammonium (NH_4^+) and lead (Pb^{2+}) appear to increase as clouds move eastward in the SoCAB. It was suggested that emissions of NH_3 (e.g. from feedlots near Riverside) and of Pb (e.g. from automobile exhausts) were transported upward into the clouds.

- Sulfate concentrations appear to increase slightly with time. However, it was not possible from the data to differentiate between the following hypotheses: formation of sulfate by aqueous oxidation of SO_2, upward transport of sulfate from below the cloud, or both.

- Nitrate concentrations appear to increase notably with time. Formation of nitrate by oxidation of NO_2 in the cloud layer appears probable.

- Calculations of the formation of aerosols from the evaporation of cloud droplets led to the result that large aerosols would be formed (about 0.5 to 1.0 um in diameter). During cloud droplet evaporation, some nitric acid and hydrochloric acid (HCl) would evaporate.

PREPARATION OF THE MODEL INPUT DATA

The data collected by Richards et al. constitute a very comprehensive set for the evaluation of a cloud model. In particular, the data collected in the 1985 field program are very complete since gas-phase hydrocarbons were also measured during this program.

Table 4-1 presents a comparison of the input data required by the model and the data base available from Richards et al. (1987).

All gas-phase concentrations are available in the clouds except H_2O_2, NH_3 and HNO_3. The latter two species, NH_3 and HNO_3, are primarily in solution and their gas-phase concentrations can be neglected. The value of the gas-phase concentration of H_2O_2 needs to be calculated from the measured aqueous-phase concentration according to Henry's law. The concentration of PAN was always below the detection limit of 0.5 ppb. Concentrations of SO_2, NO, NO_2 and O_3 which are monitored continuously, are also available below cloud base. Air samples were collected in canisters and analyzed for C_1 through C_{10} paraffins, olefins and aromatics. Concentrations of formaldehyde and acetaldehyde were measured in both the gas phase and the liquid phase. Detection limits were 1 to 2 ppb for SO_2 and 2 to 3 ppb for NO and NO_x. Uncertainties in concentrations above the detection limits were 2 to 3 ppb for SO_2, 2 to 5 ppb for NO_x and 3 to 5 ppb for NO (Richards, 1988).

Table 4-1. Input Data for the Cloud Model

Input Data	Data base of Richards et al. (1987)
Chemistry	
Gas-phase concentrations of SO_2, NO, NO_2, O_3, NH_3, H_2O_2, aldehydes, paraffins, olefins, aromatics, PAN, CO, CO_2, HNO_3.	All concentrations available in clouds except H_2O_2 (NH_3 and HNO_3 are primarily in solution). Concentrations of SO_2, NO, NO_2, and O_3 available below clouds. Background concentration of CO_2 is 345 pm.
Aqueous-phase concentrations of S(IV) (all forms of dissolved SO_2 including HMSA), S(VI), NO_3^-, NH_4^+, Na^+, K^+, Ca^{2+}, Mg^{2+}, Fe^{3+}, Mn^{2+}, Pb^{2+}, Cl^-, HCHO, CH_3CHO, H_2O_2 in clouds.	All concentrations available in clouds (however, HMSA concentration is not available).
Aerosol chemical composition (sulfate, nitrate, ammonium) and size distribution in clouds and below clouds.	Chemical composition available in clouds (however, uncertainties are associated with these data), size distribution available (above 0.09 um).
Meteorology	
Liquid water content (including cloud base and top), mean droplet radius, temperature, pressure, relative humidity below cloud, atmospheric stability, updraft velocity, rainfall rate.	All data available except the updraft velocity and rainfall rate.
Emissions	
SO_2, NO, NO_2, NH_3, hydrocarbons.	Data available from other sources (SoCAB emission inventory).

Aqueous-phase concentrations of nearly all solutes of interest were measured. No aqueous organic species concentrations were determined except formaldehyde and acetaldehyde concentrations. Species of potential interest which were not measured consist of hydroxymethane sulfonic acid (HMSA), and organic acids (formic and acetic acids). Uncertainties in the aqueous-phase concentrations were estimated to be about 5 to 10 percent (Richards, 1988).

The total S(IV) concentration was measured, however, it includes both dissolved SO_2 (i.e., H_2SO_3, HSO_3^- and SO_3^{2-}) and SO_2 complexed as HMSA.

Aerosols were measured in the clouds and their sampled chemical composition includes sulfate, nitrate and ammonium. However, these aerosols represent all suspended droplets less than about 2.5 um in diameter as selected by a cyclone inlet. For the purpose of the modeling, it was assumed that sulfate, nitrate and ammonium were primarily present in the droplets sampled with the cloud water collector which selected droplets larger than about 3 um in diameter. It should be noted that data on sulfate, nitrate, and ammonium are not available below the cloud.

Meteorological data needed for the model include the liquid water content as function of height, mean droplet radius, temperature, pressure and relative humidity vertical profiles, atmospheric stability, the updraft velocity and the rainfall rate. All these data are available except the atmospheric stability, updraft velocity and the rainfall rate. The atmospheric stability can be estimated from the vertical temperature profile. It should be noted that the liquid water content and rainfall rate can be calculated with the cloud microphysics model that is described in the following section. Therefore, one is allowed one unknown variable among the cloud physics variables. If the rainfall rate is known to be zero, it is then possible to estimate the updraft velocity from information on the temperature, pressure, relative humidity and

liquid water content. The liquid water contents were obtained from the King probe when available or from the forward scattering spectrometer probe (FSSP) otherwise. A factor of two of uncertainty was typical when comparing King probe data with FSSP data. The King probe data are believed to be more accurate than the FSSP data (Richards, 1988). Temperature and dew point temperatures were measured by the aircraft and were also available from radiosondes on certain days.

Emission data can be obtained from standard gridded emission inventories. However, these emission data are not required if the surface layer concentrations are continuously input to the model as a boundary condition.

Section 5
DESCRIPTION OF THE CLOUD MODEL

The mathematical model used in this study provides a detailed treatment of the gas-phase and aqueous-phase atmospheric chemistry and some treatment of the basic cloud transport processes. This model has been described in detail by Seigneur and Saxena (1988) and this section presents only an overview of the major features of the model.

In addition, a cloud microphysics model was used to calculate a consistent set of meteorological input data to the cloud model.

We describe first the treatment of chemical and physical atmospheric processes in the cloud model. Then, we describe the cloud microphysics model that is used as a meteorological preprocessor of the cloud model.

TRANSPORT PROCESSES

The transport processes which are treated in the cloud model include vertical transport of pollutants due to the cloud updraft, vertical and horizontal turbulent diffusion, and rainfall through the cloud and the mixing layer. A schematic representation of these transport processes is presented in Figure 5-1.

The cloud model consists of a series of layers that extend from the ground to the top of the cloud. The change in pollutant concentrations in each layer is represented mathematically by a set of partial differential equations (Seigneur and Saxena, 1988).

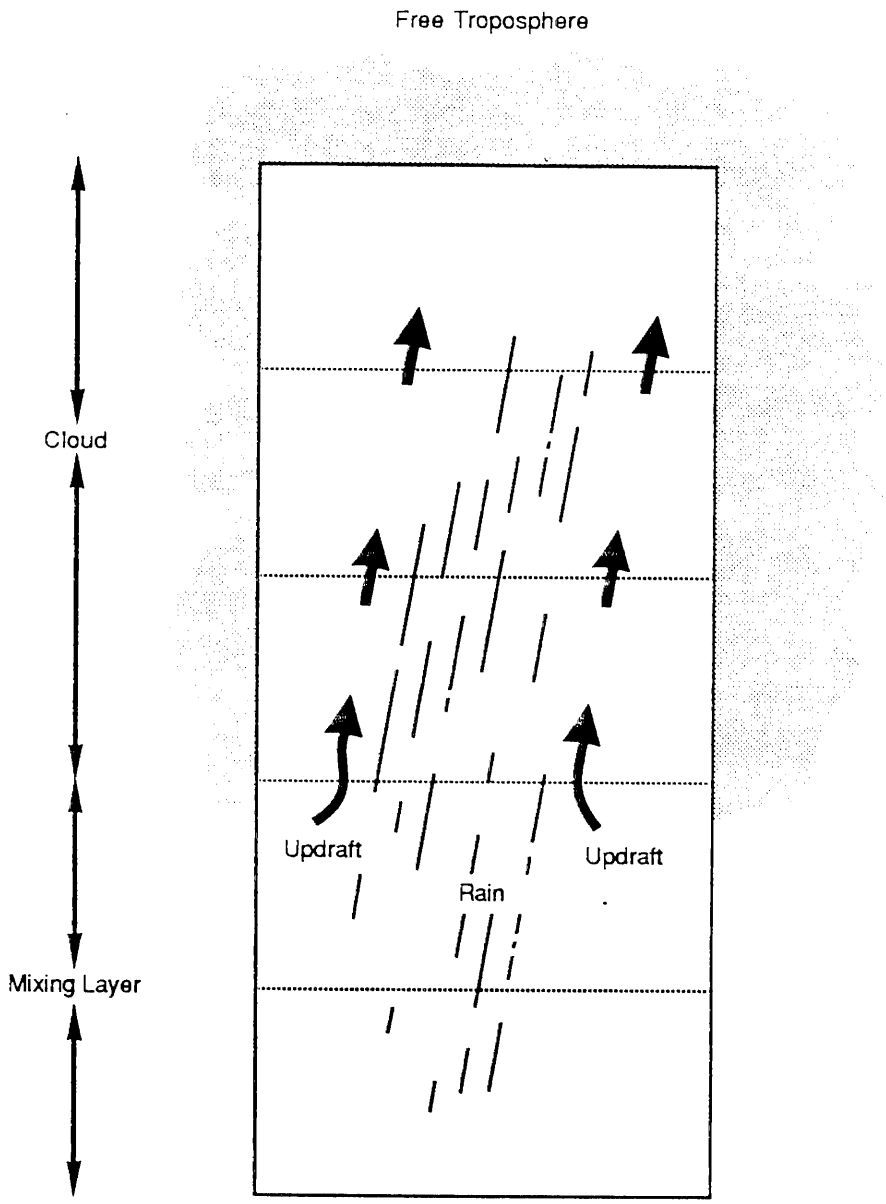

Figure 5-1 Schematic Representation of the Cloud Model

CHEMICAL KINETIC MECHANISM

The chemical kinetic mechanism consists of three major components:

1. A gas-phase chemical kinetic mechanism
2. A gas/droplet mass transfer component
3. An aqueous-phase chemical kinetic mechanism

The gas-phase chemistry is simulated according to the Carbon-Bond Mechanism IV (CBM-IV) (Whitten and Gery, 1986). A reaction was added to treat the oxidation of SO_2 by OH radicals to form H_2SO_4 and HO_2 radicals.

The chemical kinetic mechanism CBM-IV was also updated to reflect recent results reported in the literature.

Sverdrup et al. (1987) investigated the gas-phase homogeneous hydrolysis of N_2O_5 to HNO_3. This reaction is important for nighttime formation of HNO_3 under dry conditions. Sverdrup et al. (1987) reported an upper limit of 4×10^{-4} $ppm^{-1}min^{-1}$ for the rate constant of this reaction. This value was substituted to the previous value of 1.9×10^{-6} $ppm^{-1}min^{-1}$ suggested by Whitten and Gery (1986).

The gas-phase chemical kinetic mechanism consists of a set of 71 reactions among 30 chemical species. It is presented in Table 5-1.

The treatment of gas-droplet mass transfer is described by Seigneur and Saxena (1988). It includes Henry's law equilibrium at the gas-droplet interface for all species and gas-phase diffusion and droplet diffusion for radicals. Diffusion processes are assumed not to be rate limiting for molecular species. The droplets are assumed to be well mixed.

TABLE 5-1. The Carbon-Bond Mechanism IV

	Reaction		Rate constant[a]	Activation energy[b]
1	NO2	= NO +O	vary	
2	O	= O3	$4.65 \times 10^{+6}$	-690.
3	O3 +NO	= NO2	26.6	1430.
4	O +NO2	= NO	13800.	
5	O +NO2	= NO3	2320.	-600.
6	O +NO	= NO2	3120.	-411.
7	NO2 +O3	= NO3	0.0474	2450.
8	O3	= 0.205 OH + 0.897 O	vary	
9	O3	= O	0.042 X k1	
10	O3 +OH	= HO2	100.	940.
11	O3 +HO2	= OH	3.0	580.
12	NO3 +NO	= 2. NO2	28100.	-250.
13	NO3 +NO2	= NO +NO2	0.59	1230.
14	NO3 +NO2	= N2O5	1780.	60.
15	N2O5	= 2. HNO3	0.0285	
16	N2O5	= NO3 +NO2	3.12	10840.
17	NO +NO2	= 2. HNO2	2.4×10^{-7}	
18	HNO2+HNO2	= NO +NO2	1.5×10^{-5}	
19	HNO2	= NO +OH	0.18 X k1	
20	NO2 +OH	= HNO3	16300.	-560.
21	NO +OH	= HNO2	9770.	-427.

TABLE 5-1. Continued

	Reaction		Rate constant[a]	Activation energy[b]
22	HO2 +NO	= OH +NO2	12300.	-240.
23	NO +NO	= 2. NO2	1.52×10^{-4}	-530.
24	H2O2	= 2. OH	0.0014 X k1	
25	OH +H2O2	= HO2	2520.	187.
26	OH +HNO2	= NO2	9770.	
27	OH +HNO3	= NO3	192.	-778.
28	NO3	= 0.85NO2 +0.85 O +0.15NO	30.6 X k1	
29	HO2 +HO2	= H2O2	4144.	-1150.
30	HO2 +HO2	= H2O2	3270.	-5800.
31	OH +CO	= HO2	400.	
32	FORM+OH	= HO2 +CO	15000.	
33	FORM	= 2. HO2 +CO	vary	
34	FORM	= CO	vary	
35	FORM+O	= OH +HO2 +CO	237.	1550.
36	FORM+NO3	= HNO3 +HO2 +CO	0.93	
37	ALD2+O	= C2O3 +OH	636.	986.
38	ALD2+OH	= C2O3	24000.	-250.
39	ALD2+NO3	= C2O3 +HNO3	3.7	
40	ALD2	= XO2 +2.HO2 +CO +FORM	vary	
41	ALD2+HO2	= XO2 +2.FORM +HO2	5.	
42	C2O3+NO	= NO2 +XO2 +FORM +HO2	16500.	-250.
43	C2O3+NO2	= PAN	9000.	-250.
44	PAN	= C2O3 +NO2	0.0222	14000.
45	C2O3+C2O3	= 2. XO2 +2.FORM +2.HO2	3700.	
46	C2O3+HO2	=	9600.	

TABLE 5-1. Continued

	Reaction		Rate constant[a]	Activation energy[b]
47	MGLY	= C2O3 +HO2 +CO	0.02 X k1	
48	MGLY+OH	= XO2 +C2O3	26000.	
49	OH	= XO2 +FORM +HO2	21.	
50	PAR +OH	= 1.49XO2 +0.067XO2N + 0.93HO2 +0.45ALD2 -0.75PAR	1150.0	
51	O +OLE	= 0.95ALD2 +0.35HO2 + 0.20XO2 +0.15CO + 0.05FORM +0.05C2O3 + -0.35PAR	5920.	324.
52	OH +OLE	= FORM +ALD2 +XO2 +HO2 -PAR	42000.	-537.
53	O3 +OLE	= 0.5ALD2 +0.66FORM + 0.212CO +0.28HO2 + 0.144XO2 +0.08 OH -PAR	0.018	1897.
54	NO3 +OLE	= 0.91XO2 +0.91HO2 + 0.09XO2N	11.4	
55	O +ETH	= FORM +XO2 +CO +2.HO2	1080.	800.
56	OH +ETH	= XO2 +2.FORM +HO2	12000.	-382.
57	O3 +ETH	= FORM +0.37CO + 0.13HO2	0.0027	2840.
58	TOL +OH	= HO2 +0.64XO2 +1.13FORM + 0.56MGLY +0.36PHEN + 0.36PAR +1.13CO	9750.	
59	PHEN+NO3	= PHO +HNO3	14000.	
60	PHO +NO2	=	20000.	
61	XYL +OH	= HO2 +0.72XO2 +0.67CO + 1.33MGLY +0.28PHEN + 0.56PAR +0.06TLA + 0.67FORM	36000.	
62	TLA +OH	= XO2 +PHO +2. PAR	20000.	
63	ISOP+O	= HO2 +0.8ALD2 +0.55OLE + 0.5XO2 +0.5CO + 0.45ETH -0.1PAR	28000.	

TABLE 5-1. Continued

Reaction			Rate constant[a]	Activation energy[b]
64 ISOP+OH	=	0.87XO2 +0.87FORM + 0.87HO2 +0.29PAR 0.29OLE +0.58ETH 0.29ALD2	126000.	
65 ISOP+O3	=	FORM +0.45ALD2 + 0.55ETH +0.98HO2 + 0.100LE +0.60CO -0.25PAR	0.018	
66 ISOP+NO3	=	XO2N	165.	
67 XO2N+NO	=		1000.	
68 XO2 +NO	=	NO2	12000.	
69 XO2 +HO2	=		5000.	-1300.
70 XO2 +C2O3	=	XO2 +HO2 +FORM	2400.	
71 SO2 +OH	=	H2SO4 +HO2	1500.	

a All rate constants are in approriate ppm and min units at 298K and one atmosphere of air. That is all unimolecular and photolysis reactions (+hv) are in units of min^{-1}; all bimolecular reactions are in units of ppm^{-1} and min^{-1}; and all termolecular reactions are in units of ppm^{-2} min^{-1}. Rate constants designated as "vary" are defined in Whitten, Killus, and Johnson (1985a and b).

b The numbers listed are Arrhenious temperature coefficients in degrees Kelvin for B in the expression $k_T = k_{298} \exp(B \times (\frac{1}{298} - \frac{1}{T}))$.

The aqueous-phase chemical kinetic mechanism is described by Seigneur and Saxena (1988). It consists in a set of 18 gas/droplet equilibria, 13 ionic equilibria, 2 hydration equilibria and 30 chemical reactions. This mechanism treats the aqueous formation of sulfate and nitrate as well as radical chemistry. It is presented in Tables 5-2 and 5-3.

This aqueous-phase mechanism was updated to reflect recent kinetic and mechanistic results on the aqueous chemistry of sulfate and nitrate formation.

Huie and Neta (1987) reported recent measurements of the reaction kinetics of the oxidation of S(IV) by OH radicals. The rate constants of the reaction OH with HSO_3^- and SO_3^{2-} were 5.7×10^{11} $M^{-1}min^{-1}$ and 3.3×10^{11} $M^{-1}min^{-1}$, respectively (Seigneur and Saxena, 1988). The new values are 2.7×10^{11} $M^{-1}min^{-1}$ and 3.1×10^{11} $M^{-1}min^{-1}$, respectively.

Several recent studies on the oxidation of S(IV) by O_2 catalyzed by iron and manganese have been reported. Martin and Hill (1987) investigated the iron catalyzed oxidation of S(IV). They reconciled various rates reported in the literature by taking into account the effect of ionic strength, sulfate concentration and initial S(IV) concentration. Their rate expression at pH below 3.6 is first-order in Fe and S(IV) concentrations and inversely proportional to the H^+ concentration.

Martin and Hill (1988) measured the effect of ionic strength on the rate of the oxidation of S(IV) catalyzed by manganese at different concentrations of S(IV). An increase in ionic strength tends to inhibit the reaction rate. At low S(IV) concentrations (i.e., below 10^{-6}M), the reaction rate is first-order in both Mn and S(IV) concentrations. At high S(IV) concentrations (i.e., above 10^{-4}M), the reaction rate is second-order in Mn concentration and zeroth-order in S(IV) concentration.

TABLE 5-2. Equilibrium reactions with temperature dependence.*

Equilibrium Reaction	$K^{\dagger}_{298}$	$\frac{-\Delta H}{R}^{\S}$	Reference
$SO_2(g) \rightleftharpoons SO_2(aq)$	1.23	3,020	Smith and Martell (1976)
$SO_2(aq) \rightleftharpoons HSO_3^- + H^+$	1.23×10^{-2}	2,010	Smith and Martell (1976)
$HSO_3^- \rightleftharpoons SO_3^{2-} + H^+$	6.6×10^{-8}	1,510	Smith and Martell (1976)
$O_3(g) \rightleftharpoons O_3(aq)$	1.13×10^{-2}	2,300	Kosak-Channing and Helz (1983)
$H_2O_2(g) \rightleftharpoons H_2O_2(aq)$	7.1×10^{4}	6,800	Martin and Damschen (1981)
$HNO_3(g) \rightleftharpoons HNO_3(aq)$	2.1×10^{5}	8,700	Schwartz and White (1981)
$HNO_3(aq) \rightleftharpoons NO_3^- + H^+$	15.4		Schwartz and White (1981)
$HNO_2(g) \rightleftharpoons HNO_2(aq)$	49.	4,800	Schwartz and White (1981)
$HNO_2(aq) \rightleftharpoons NO_2^- + H^+$	5.1×10^{-4}	-1,260	Schwartz and White (1981)
$NO_2(g) \rightleftharpoons NO_2(aq)$	6.4×10^{-3}	2,500	Lee and Schwartz (1981); NBS (1965)
$NO(g) \rightleftharpoons NO(aq)$	1.9×10^{-3}	1,480	Schwartz and White (1981)
$CO_2(g) \rightleftharpoons CO_2(aq)$	3.4×10^{-2}	2,420	Smith and Martell (1976); NBS (1965)
$CO_2(aq) \rightleftharpoons HCO_3^- + H^+$	4.5×10^{-7}	-1,000	Smith and Martell (1976)
$HCO_3^- \rightleftharpoons CO_3^{2-} + H^+$	4.7×10^{-11}	-1,760	Smith and Martell (1976)
$OH(g) \rightleftharpoons OH(aq)$	25.0	5,200	Klaning et al. (1985)
$HO_2(g) \rightleftharpoons HO_2(aq)$	2.0×10^{3}	6,600	Schwartz (1984)
$NO_3(g) \rightleftharpoons NO_3(aq)$	2.1×10^{5}	8,700	Jacob (1986)

TABLE 5-2. Concluded.

Equilibrium Reaction	$K_{298}^{\dagger}$	$\frac{-\Delta H}{R}^{\delta}$	Reference
$H_2O \rightleftarrows H^+ + OH^-$	1.0×10^{-14}	-6,710	Smith and Martell (1976)
$NH_3(g) \rightleftarrows NH_3(aq)$	75.	3,400	Hales and Drewes (1979)
$NH_3(aq) \rightleftarrows NH_4^+ + OH^-$	1.75×10^{-5}	-450	Smith and Martell (1976)
$PAN(g) \rightleftarrows PAN(aq)$	2.9	5,910	Lee (1984a)
$H_2SO_4(aq) \rightleftarrows HSO_4^- + H^+$	1,000.	--	Perrin (1982)
$HSO_4 \rightleftarrows SO_4^{2-} + H^+$	1.0×10^{-2}	2,720	Smith and Martell (1976)
$HCHO(g) \rightleftarrows CH_2(OH)_2(aq)$	6.3×10^3	6,500	Ledbury and Blair (1925)
$HCHO(g) \rightleftarrows HCHO(aq)$	3.46	--	Hoffman and Calvert (1985)
$CH_3CHO(g) \rightleftarrows CH_3CHO(aq)$	13	5.5	Snider and Dawson (1985)
$CH_3CHO(aq) \rightleftarrows CH_3CH(OH)_2(aq)$	1.2	2.5	Bell (1966)
$HC\ell(g) \rightleftarrows HC\ell(aq)$	1.1	2,020	Marsh and McElroy (1985)
$HC\ell(aq) \rightleftarrows H^+ + C\ell^-$	1.7×10^{-6}	6,900	Marsh and McElroy (1985)
$CH_3O_2H(g) \rightleftarrows CH_3O_2H(aq)$	1.0×10^3	--	Hoffmann and Calvert (1985)
$CH_3COO_2H(g) \rightleftarrows CH_3COO_2H(aq)$	1.0×10^4	--	Hoffmann and Calvert (1985)
$HO_2(aq) \rightleftarrows H^+ + O_2^-$	3.5×10^{-5}	--	Perrin (1982)
$H_2O_2(aq) \rightleftarrows HO_2^- + H^+$	2.2×10^{-12}	-3,730	Smith and Martell (1976)

* The temperature dependence is represented by

$K = K_{298} \exp\left[\frac{-\Delta H}{R}\left(\frac{1}{T} - \frac{1}{298}\right)\right]$ where K is equilibrium constant at temperature T (in Kelvin)

† Units of K and K_{298} are dimensionless, M or M atm^{-1}

δ $\frac{-\Delta H}{R}$ is in Kelvin

TABLE 5-3. **Aqueous phase kinetics.**

No.	Reaction*	Rate Expression†	Rate Constant§ k_{298}	Rate Constant§ $-E/R$	Reference
1	$S(IV) + H_2O_2 \rightarrow S(VI) + H_2O$	$\frac{k_0[H_2O_2][SO_2]}{1. + 16[H^+]}$	7.6×10^7	-4,430	McArdle and Hoffmann (1983)
2	$S(IV) + O_3 \rightarrow S(VI) + O_2$	$\left(k_0[SO_2] + k_1[HSO_3^-] + k_2[SO_3^{2-}]\right)[O_3]$	1.44×10^6 2.22×10^7 9.00×10^{10}	-- -5,530 -5,280	Hoffmann and Calvert (1985)
3a	$S(IV)(+\frac{1}{2}O_2) \xrightarrow{Mn^{2+}} S(VI)$	$S(IV) > 10^{-4}M$ $k_0\,[Mn^{2+}]^2$ $S(IV) < 10^{-4}M$ $k_1\,[Mn^{2+}]\,[S(IV)]$	$4 \times 10^4 f(I)$** $6 \times 10^4 f(I)$	-13,700 -13,700	Martin and Hill (1988)
3b	$S(IV)\ (+\frac{1}{2}O_2) \xrightarrow{Fe^{3+}} S(VI)$	$k_2\frac{[Fe^{3+}]}{[H^+]}\,[S(IV)]$	360 g (I , [S(IV)])††	-11,000	Martin and Hill (1987)
4	$HSO_3^- + OH\ (+HSO_3^- + O_2) \rightarrow SO_4^{2-} + SO_4^- + H^+ + H_2O$	$k_0[OH][HSO_3^-] + k_1[OH][SO_3^{2-}]$	2.7×10^{11} 3.1×10^{11}	-- --	Huie and Neta (1987)
5	$SO_4^- + H_2O_2 \rightarrow HSO_4^- + HO_2$	$k_0[SO_4^-][H_2O_2]$	7.2×10^8	--	Ross and Neta (1979)
6a	$S(IV) + N(III) \rightarrow S(VI) + \frac{1}{2}N_2O$	pH < 3; $k_0([HNO_2] + [NO_2^-])[S(IV)][H^+]^{0.5}$	8.52×10^3	--	Martin et al. (1981); Martin (1984)
6b	$2HSO_3^- + NO_2^- \rightarrow HON(SO_3)_2^{2-} + OH^-$	pH > 3 $k_1[NO_2^-][HSO_3^-][H^+]$	2.86×10^5	-6,100	Oblath et al. (1981)

TABLE 5-3. Continued.

No.	Reaction*	Rate Expression†	Rate Constant§ k_{298}	Rate Constant§ $-E/R$	Reference
7	$S(IV) + PAN \rightarrow S(VI)$	$\frac{k_0[PAN][HSO_3^-]}{[H^+]}$	0.4	—	Lee (1984a)
8	$HSO_3^- + CH_3O_2H \rightarrow SO_4^{2-} + H^+ + CH_3OH$	$k_0[H^+][CH_3O_2H][HSO_3^-]$	1.43×10^9	−3800	Hoffmann and Calvert (1985)
9	$HSO_3^- + CH_3COO_2H \rightarrow SO_4^{2-} + H^+ + CH_3CO_2H$	$(k_0[H^+] + k_1)[HSO_3^-][CH_3COO_2H]$	3.02×10^9 3.6×10^4	−4000 —	Hoffmann and Calvert (1985)
10	$S(IV) + HO_2 \rightarrow S(VI) + OH$	$k_0[HO_2][HSO_3^-] + k_1[O_2^-][SO_3^{2-}]$	6×10^7 6×10^6	— —	Hoffmann and Calvert (1985)
11§	$2NO_2 + HSO_3^-(+H_2O) \rightarrow 3H^+ + 2NO_2^- + SO_4^{2-}$	$k_0[S(IV)][NO_2]$	1.2×10^8	—	Lee and Schwartz (1983); Lee (1984a)
12	$NO_3 + Cl^- \rightarrow NO_3^- + Cl$	$k_0[NO_3][Cl^-]$	6×10^9	—	Chameides (1984)
13	$NO_3 + HSO_3^-(+HSO_3^- + O_2) \rightarrow NO_3^- + 2H^+ + SO_4^- + SO_4^{2-}$	$k_0[NO_3][HSO_3^-]$	6×10^9	—	Chameides (1984)
14	$NO_3 + H_2O_2 \rightarrow NO_3^- + H^+ + HO_2$	$k_0[NO_3][H_2O_2]$	6×10^7	—	Chameides (1984)
15	$2NO_2(+H_2O) \rightarrow 2H^+ + NO_2^- + NO_3^-$	$k_0[NO_2]^2$	4.2×10^9	—	Schwartz (1984b)
16	$PAN \rightarrow NO_3^-$	$k_0[PAN]$	2.4×10^{-2}	—	Lee (1984b)
17	$NO_2 + O_3 \rightarrow NO_3^- + O_2$	$k_0[O_3][NO_2^-]$	3.0×10^7	—	Damschen and Martin (1983)
18	$HNO_2 + H_2O_2 \xrightarrow{H^+} HNO_3 + H_2O$	$k_0[H_2O_2][HNO_2][H^+]$	2.8×10^5	—	Damschen and Martin (1983)
19	$O_3 + H_2O_2 \rightarrow H_2O + 2O_2$	$k_0[O_3]^{0.5}[H_2O_2]$	0.47	—	Martin *et al.* (1983); Bray (1938); Taube and Bray (1940)
20	$OH + H_2O_2 \rightarrow HO_2 + H_2O$	$k_0[OH][H_2O_2]$	1.6×10^9	−1700	Christensen *et al.* (1982)
21	$2HO_2 \rightarrow H_2O_2 + O_2$	$k_0[HO_2]^2$	4.5×10^7	—	Behar *et al.* (1970)
22	$H_2O_2 \xrightarrow{h\nu} 2OH$	$k_0[H_2O_2]$	$f(h\nu)$	—	Livingston and Zeldes (1966); Graedel and Weschler (1981)
23	$O_3 + HO_2^- \rightarrow OH + O_2^- + O_2$	$k_0[O_3][HO_2^-]$	1.7×10^8	—	Staehelin and Hoigne (1982)
24	$O_3 + OH^- \rightarrow HO_2 + O_2^-$	$k_0[O_3]^{1.5}[OH^-]$	4.8×10^6	—	Haruta and Takeyama (1981)
25	$O_3 + HO_2 \rightarrow OH + 2O_2$	$k_0[O_3][HO_2]$	2.4×10^8	—	Chameides and Davis (1982)
26	$O_3 + OH \rightarrow HO_2 + O_2$	$k_0[O_3][OH]$	1.8×10^{11}	—	Bahnemann and Hart (1982)
27	$HCHO + HSO_3^- \rightarrow HMSA$	$(k_0[HSO_3^-] + k_1[SO_3^{2-}])[HCHO]$	4.74×10^4 1.49×10^9	−3000 −2450	Boyce and Hoffmann (1984)
28	$HMSA + OH^- \rightarrow SO_3^{2-} + HCHO + H_2O$	$k_0[HMSA][OH^-]$	2.16×10^5	—	Munger *et al.* (1986)
29	$HO_2 + O_2^-(+H_2O) \rightarrow H_2O_2 + O_2 + OH^-$	$k_0[HO_2][O_2^-]$	6.0×10^9	−1500	Bielski (1978)
30	$O_3 + O_2^-(+H_2O) \rightarrow OH + 2O_2 + OH^-$	$k_0[O_3][O_2^-]$	9.0×10^{10}	−1500	Bielski (1978)

Notes

* All species and concentrations pertain to aqueous phase.

** $f(I) = 10^{-4.07} \sqrt{I}/(1+\sqrt{I})$ where I is the ionic strength

† The rate is in M min^{-1}

†† $g(I, S(VI)) = \frac{10^{-2.0} \sqrt{I}/(1+\sqrt{I})}{1+150\,[S(VI)]^{2/3}}$

‡ $k = k_{298} \exp\left[\frac{-E}{R}\left(\frac{1}{T} - \frac{1}{298}\right)\right]$ where k_{298} is reaction rate at 298 K and T is temperature in K. For each reaction, the values of k_0, k_1, k_2 etc. are presented in the same order.

§ This reaction is only included for pH > 5.

Ibusuki and Takeuchi (1987) studied the oxidation of S(IV) catalyzed by manganese and iron under conditions typical of the polluted atmospheric environment. They demonstrated the existence of synergism between the two catalysts and quantified the pH dependence of the reaction rates at 24°C and the temperature dependence of the reaction rates at a pH of 4.2. Their determination of the rate constant of the reaction catalyzed by iron agrees with the value originally reported by Martin (1984) at pH=4.

The mechanisms of Martin and Hill (1987, 1988) were selected to represent the oxidation of S(IV) by O_2 when catalyzed by iron and manganese. No expression was suggested by Martin and Hill for synergism between iron and manganese catalysis. The expression proposed by Ibusuki and Takeuchi (1987) for synergism between iron and manganese catalysis is not consistent with the formulations used by Martin and Hill (1987, 1988). Therefore, we did not incorporate any treatment of the synergistic effects of iron and manganese catalysis of aqueous oxidation of S(IV).

CLOUD MICROPHYSICS

The simulation of the cloud microphysics consists in the calculation of the distribution of water between four phases:

(1) vapor

(2) cloud droplets

(3) rain drops

(4) ice particles (or snow)

Cloud dynamics is not simulated and only a kinematic treatment of transport phenomena is provided. The inputs to the model include the following:

- updraft velocity as function of altitude
- temperature as function of altitude

- pressure as function of altitude
- total water content as function of altitude.

Transport occurs through vertical motions due to the updraft and precipitation of rain drops and ice particles. If the updraft velocity varies with height, entrainment or detrainment between the cloud and its environment will take place to satisfy the continuity equation.

The treatment of liquid water microphysics in the model follows the formulation of Kessler (1969). The treatment of ice particles and snow is based on the model of Koenig and Murray (1976).

Within a given layer of the model, the total water content Q_w is the sum of the mixing ratios of water vapor, cloud droplets, rain drops and ice. The changes in the individual mixing ratios are calculated in two steps. First, the changes within each layer due to microphysical processes are calculated. Second, the changes due to mass transport are calculated.

The changes due to microphysical processes follow the diagram presented in Figure 5-2.

Rain drops and cloud droplets are assumed to have a Marshall-Palmer size distribution. Clearly, evaporation of cloud droplets does not take place when condensation on cloud droplets occurs, and vice-versa. Riming, vapor diffusion to ice particles and nucleation of ice particles only take place below 0°C. Melting and sublimation of ice only take place above 0°C. Riming occurs first from rain drops, then, from cloud droplets.

The cloud transport processes that affect the water mixing ratios include updraft, precipitation and entrainment or detrainment from the sides of the cloud.

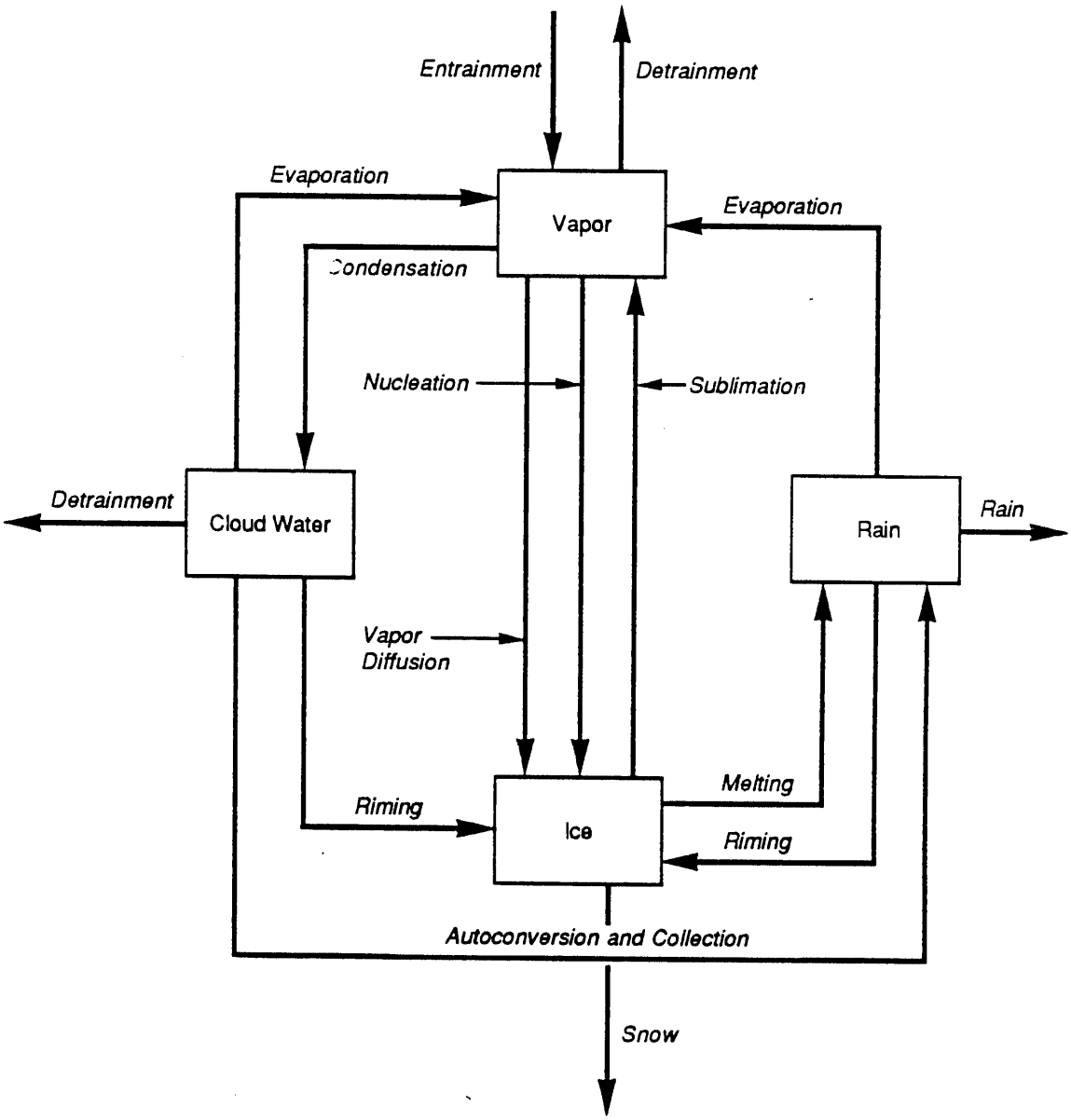

Figure 5-2 Schematic Description of the Cloud Microphysical Processes

The entrainment/detrainment term is calculated from the vertical variation in the updraft velocity and allows mass conservation of the air mass. Entrainment occurs only for water vapor. Detrainment occurs for species assumed to have a fall velocity of zero, i.e., water vapor and cloud droplets. The fall velocities of rain drops and ice particles are calculated according to the formulation of Wobus et al. (1971).

It may be noted that if the distribution of water between the four phases (i.e, vapor, cloud droplets, rain drops, and ice) is known, then, it is possible to apply the cloud microphysics model to the determination of one of the input data such as the updraft velocity. This mode of application may be particularly useful since measurements of liquid water content, precipitation and relative humidity are generally available more readily than updraft velocities.

SECTION 6
EQUILIBRIUM CHEMISTRY

INTRODUCTION

Equilibrium chemistry consists of gas-phase/aqueous-phase equilibria and aqueous-phase ionic and hydration equilibria. Clearly, it is essential that these equilibria be properly treated in a model since they determine the aqueous-phase concentrations of the chemical species at a given time and govern the rates of aqueous-phase chemical kinetics. The experimental data collected by Richards et al. (1983a, 1985, 1987) constitute an excellent data set for the evaluation of the treatment of equilibrium chemistry by the model because all major aqueous-phase species were measured.

An overall evaluation of the equilibrium chemistry is performed by comparing the measured and calculated pH values. The pH is not an input to the model and it is calculated from the condition that the electroneutrality of the solution be satisfied. This electroneutrality condition requires solving all gas-phase/aqueous-phase equilibria and aqueous-phase ionic and hydration equilibria by iteration until the concentrations of cations and anious become equal.

If the calculated and measured pH values are in close agreement, it may be assumed that the model treats correctly the equilibrium chemistry. If there is a discrepancy between the calculated and measured pH values, there are two possible explanations:

1. The model fails to treat one or more equilibria correctly which leads to erroneous concentrations of some ions.

2. The experimental data are incomplete or inaccurate and do not provide an adequate input data set for the model calculations.

More specific evaluation of equilibrium chemistry can be performed when concentrations of several species involved in an equilibrium are available. This is the case for example when both gas-phase and aqueous-phase concentrations of a species are available.

We present and discuss in this section the results of the model performance evaluation for equilibrium chemistry. We first present the comparison of measured and calculated pH values. Then, we analyze the equilibrium chemistry of S(IV) and aldehydes.

CLOUD DROPLET PH

The cloud droplet pH was calculated for a total of 52 cases, including 10 cases from the 1981 data, 11 cases from the 1982 data, 8 cases from the 1984 data, and 23 cases from the 1985 data. Cases for which data on anion and cation concentrations were significantly incomplete were not considered.

Measurements of S(IV) in the aqueous phase did not differentiate between dissolved SO_2, i.e., H_2SO_3, HSO_3^- and SO_3^{2-} and SO_2 complexed with HCHO as hydroxymethane sulfonic acid (HMSA). Therefore, we performed two types of simulations. In the first type of simulation, we assumed that measured S(IV) was present as HSO_3^- and no HMSA was present. In the second type of simulation, we assumed that H_2SO_3, HSO_3 and SO_3^{2-} were in equilibrium with the measured SO_2 gas-phase concentration and that the remaining measured S(IV) concentration corresponded to HMSA.

The calculated pH values are listed and compared with the measured pH values in Table 6-1. The normalized bias and absolute error in the H^+ concentrations are presented in Table 6-2 for each year of data. Overall, there is a bias toward the underprediction of the H^+ concentration. The 1981 data set with HMSA and the 1984 data set are the only ones that show a trend toward overprediction of the

Table 6-1. Comparison of Calculated and Measured pH Values at Equilibrium

Case			pH Value		$[H^+]$
Number	Date	Tape/Pass	Calculated(2)	Measured	Normalized Difference (1,2) (%)
1	11-23-81(3)	296/1	3.81/3.81	3.56	-44/-44
2	11-23-81(4)	296/2	3.89/3.85	3.36	-70/-68
3	11-23-81(4)	296/4	3.71/3.67	3.80	+23/+35
4	11-23-81	296/5	2.94/2.91	3.05	+28/+38
5	11-24-81	296/6	2.91/2.86	2.98	+18/+32
6	11-24-81	296/7	2.91/2.89	3.02	+28/+35
7	11-24-81(3)	296/8	3.63/3.63	3.68	+12/+12
8	11-24-81(3)	297/2	3.20/3.20	3.18	-5/-5
9	11-24-81	297/3	3.68/3.62	3.72	+9/+26
10	11-24-81(4)	297/5	3.84/3.76	3.67	-32/-19
11	05-20-82	301/2	3.09/3.09	2.99	-21/-21
12	05-21-82	302/1	2.37/2.37	2.40	+6/+6
13	05-21-82	302/3	2.61/2.58	2.72	+29/+38
14	05-22-82	302/5	4.17/3.58	3.39	-84/-35
15	05-22-82	302/7	2.49/2.48	2.56	+18/+20
16	05-22-82	302/9	2.53/2.52	2.65	+33/+35
17	05-22-82	302/11	2.53/2.52	2.69	+44/+48
18	05-23-82(4)	303/5	3.21/3.19	3.05	-30/-28
19	05-23-82(4)	303/7	3.57/3.57	3.38	-36/-36
20	05-23-82(4)	303/8	3.63/3.59	3.33	-50/-45
21	05-23-82(4)	303/9	3.64/3.62	3.59	-10/-7
22	06-03-84(4)	379/1	2.94	2.96	+5
23	06-03-84(4)	379/4	2.94	2.96	+5
24	06-03-84(6)	379/6	2.68	2.70	+5
25	06-04-84	380/1-3	2.84	2.87	+7
26	06-04-84	380/4-5	2.80	2.83	+7
27	06-05-84(4)	381/1	2.95	2.96	+3
28	06-05-84(4)	381/2	3.18	3.20	+5
29	06-05-84(4)	381/3	3.61	3.60	-2
30	05-21-85(5)	432/2	3.46	3.41	-10
31	05-21-85(3)	432/3	3.36	3.35	-3
32	05-21-85	432/4	2.83	2.90	+17
33	05-21-85(4)	432/5	3.19	3.12	-14

Table 6-1. Comparison of Calculated and Measured pH Values at Equilibrium

Case			pH Value		$[H^+]$ Normalized Difference (1),(2) (%)
Number	Date	Tape/Pass	Calculated(2)	Measured	
34	05-24-85(4)	433/1-2	3.45	3.43	-5
35	05-24-85(4)	433/4	3.01	2.97	-9
36	05-24-85(6)	433/4	2.99	2.98	-3
37	05-25-85(3)	434/2	3.36	3.26	-21
38	05-25-85	434/2	3.26	3.26	-1
39	05-25-85(4)	434/3	3.25	3.25	-1
40	05-25-85(3)	434/3	3.41	3.40	-2
41	05-25-85(3)	434/4	3.38	3.37	-3
42	05-25-85	434/4	3.37	3.35	-4
43	05-26-85(3)	435/2	3.40	3.35	-12
44	05-26-85	435/3	3.33	3.31	-5
45	05-26-85(3)	435/4	3.80	3.65	-30
46	05-27-85(6)	436/2	3.39	3.32	-14
47	05-27-85(3)	436/3	3.16	3.14	-4
48	05-27-85(3)	436/4	3.64	3.42	-40
49	06-10-85(6)	440/2	3.86	3.82	-9
50	06-10-85(6)	440/3	3.25	3.20	-10
51	06-10-85(3)	440/4	3.36	3.25	-21
52	06-10-85(3)	440/5	3.20	3.60	+154

(1) The normalized difference is defined as ($[H^+]$ calculated - $[H^+]$ measured)/$[H^+]$ measured.

(2) The first value in the 81 and 82 data corresponds to no HMSA; the second value corresponds to $SO_2(g)/HSO_3^-$ equilibrium and HMSA. There was no difference between both calculations for the 84 and 85 data.

(3) S(IV) not measured, HSO_3^- calculated.

(4) $SO_2=0$ $HSO_3^-=0$, all S(IV) assumed to be HMSA.

(5) HSO_3^- concentrations exceed measured S(IV) concentrations.

(6) $SO_2=0$ and S(IV) not detected or not measured.

Table 6-2
Normalized Bias and Absolute Error in H^+ Concentrations (a)

Data Set	Normalized Bias(%)(b)	Normalized Absolute Error (%)(c)	Number of Samples
1981	-3 (+4)	27 (31)	10
1982	-9 (-2)	33 (29)	11
1984	+5	5	8
1985	-2	17	23
1985 (without case 52)	-9	10	22
All data	-3 (0.2)	20 (20)	52

(a) The first value corresponds to simulations where no HMSA was assumed to be present; the value in parentheses corresponds to simulations where HMSA was assumed to be present.

(b) The normalized bias is defined as $\frac{1}{N}\sum_{i=1}^{N}[([H^+]_{i,c} - [H^+]_{i,m})/[H^+]_{i,m}]$ where N is the number of data pairs, and subscripts c and m refer to calculated and measured values, respectively.

(c) The normalized absolute error is defined as

$$\frac{1}{N}\sum_{i=1}^{N}[\,|[H^+]_{i,c} - [H^+]_{i,m}|/[H^+]_{i,m}\,]$$

H^+ concentration. Among the 52 cases considered, the H^+ concentration is underpredicted 32 times and overpredicted 20 times. The calculated H^+ concentration is within a factor of 1.5 of the measured value 45 times out of 52; it is within a factor of 2, 49 times out of 52. The largest discrepancies occur for case 2 (11-23-81) where the H^+ concentration is underpredicted by 70 percent, case 14 (05-22-82) where it is underpredicted by 84 percent and case 52 (06-10-85) where it is overpredicted by 154 percent. If case 52 is discarded as an outlier from the 1985 data set, there is a clear trend toward underpredicting the H^+ concentration in this data set by about 9 percent.

The use of HMSA in the equilibrium calculations for the 1981 and 1982 data leads to higher H^+ concentrations (i.e., lower pH values) since the anion concentration is higher. (If no HMSA is assumed, a large fraction of the input HSO_3^- concentration is redistributed into the gas phase). Consequently, the bias shows less underprediction (or more overprediction) of the H^+ concentration. Overall, however, the absolute error is not affected by the assumption made for S(IV). It should be noted that only the cases where the measured S(IV) concentration constitutes a significant amount of the measured anion concentration show sensitivity to the HMSA assumption. There are about only 8 such cases (Cases 3, 4, 5, 6, 9, 10, 13 and 14).

EQUILIBRIUM CHEMISTRY OF S(IV)

The concentrations of S(IV) where highest in 1981 and 1982. The use of gas in power plants the following years led to small S(IV) concentrations. According to our chemical kinetic mechanism, S(IV) may be present in the aqueous phase as dissolved SO_2, i.e. H_2SO_3, HSO_3 or SO_3^{2-} or as a complex formed by reaction with HCHO. This complex, hydroxymethane sulfonic acid (HMSA), is formed by reaction of HCHO with HSO_3. Its decomposition is function of pH and occurs more slowly than its formation; at low pH, HMSA may, therefore, act as a reservoir of S(IV) in solution. At

the pH values observed in the SoCAB stratus clouds, dissolved SO_2 is primarily in the form of HSO_3^-. Therefore, S(IV) is present as HSO_3^- or HMSA.

The experimental data do not differentiate between HSO_3^- or HMSA since S(IV) in solution is stablized by reaction with HCHO before analysis. Because the decomposition rate of HMSA is slow compared to its formation rate, HMSA cannot be assumed to be in equilibrium with HSO_3^- and HCHO and the formation and decomposition reactions must be treated explicitly in the mechanism. Therefore, the presence of HMSA cannot be calculated by the equilibrium chemistry but must be assumed as an input.

Table 6-3 presents a comparison of measured and calculated S(IV) concentrations for the 18 cases for which S(IV) concentrations were measured. Cases from the 1985 field program were not included because the measured SO_2 concentrations were less than 1 ppb and were, therefore, zero within the measurement uncertainty. The calculated values represent HSO_3^- concentrations that were calculated from the equilibrium with the gas-phase SO_2 concentrations. It appears clearly that the calculated HSO_3^- concentrations are consistently less than the measured S(IV) concentrations. On the average, the calculated HSO_3^- concentrations are less than the measured HSO_3^- concentrations by factors of 3500 and 2200 for the 1981 and 1982 data. Since high concentrations of SO_2(g) and HCHO are present in many of the 1981 and 1982 cases, it appears reasonable to assume that HMSA was formed and acted as a reservoir of S(IV) in solution because of its low decomposition rate.

A possible scenario for the chemistry of S(IV) in SoCAB stratus clouds is as follows. SO_2 is emitted from a large source. The SO_2 plume mixes into stratus clouds where SO_2 reacts rapidly in cloud droplets with H_2O_2 to form sulfate and with HCHO to form

Table 6-3

Comparison of Measured and Calculated S(IV) Concentrations

Case				
Number	Date	Tape/Pass	Measured S(IV) Concentration (μM)	Calculated HSO_3^- Concentration (μM)(1)
2	11/23/81	296/2	41	.061/0
3	11/23/81	296/4	21	.027/0
4	11/23/81	296/5	89	.007/.006
5	11/24/81	296/6	129	.380/.342
6	11/24/81	296/7	89	.197/.182
9	11/24/81	297/3	30	.047/.039
10	11/24/81	297/5	27	.003/0
11	05/20/82	301/2	11	.098/.095
12	05/21/82	302/1	52	.062/.061
13	05/21/82	302/3	182	.536/.497
14	05/22/82	302/5	365	23.8/5.99
15	05/22/82	302/7	29	.045/.044
16	05/22/82	302/9	33	.035/.034
17	05/22/82	302/11	51	.122/.117
18	05/23/82	303/5	18	.001/0
19	05/23/82	303/7	5	.004/0
20	05/23/82	303/8	10	.010/0
21	05/23/82	303/9	10	.024/0

(1) The first concentration represents the calculation assuming no HMSA, the second concentration represents the calculation assuming HMSA formation. The difference in the HSO_3^- concentration results from the difference in pH.

HMSA. The SO_2 concentration is then rapidly depleted through reaction with H_2O_2 and HCHO as well as through atmospheric dispersion. As the SO_2 concentration decreases, HMSA starts to decompose back into its precursors HSO_3^- and HCHO; however, this rate is slow at the low pH values observed in the SoCAB clouds and S(IV) is, therefore, trapped in the form of HMSA. Concentrations of H_2O_2(aq) exceed S(IV) but, since most S(IV) is, then, present as HMSA, no further reaction of H_2O_2 (aq) with S(IV) takes place in significant amount. This scenario was used by Richards et al. (1983b) to explain their 1981 and 1982 data. The results of our equilibrium chemistry calculations are consistent with this hypothesis. This scenario will be simulated through a kinetic simulation in Section 9 to confirm the hypothesis advanced here.

EQUILIBRIUM CHEMISTRY OF ALDEHYDES

Measurements of formaldehyde and acetaldehyde were performed in both the interstitial gas phase and in the cloud droplet aqueous phase during the 1985 field program. These measurements allow us to test the treatment of the equilibrium chemistry of aldehydes in the model.

Table 6-4 presents a comparison of measured and calculated aldehyde concentrations in the aqueous phase. The calculated concentrations were obtained by calculating the gas-phase/aqueous-phase equilibrium and hydration equilibrium using the total (gas-phase and aqueous-phase) concentration as input to the model.

It appears that the agreement is reasonably good for formaldehyde. The calculated aqueous HCHO concentration is consistently higher than the measured value. The calculated value ranges from 1.03 to 2.13 times the measured value with an average bias of 60 percent toward overprediction. Formaldehyde is primarily present (about 99.98%) in its hydrated form $H_2C(OH)_2$.

Table 6-4

Comparison of Measured and Calculated

Aldehyde Concentrations

Case		Formaldehyde Aqueous Concentration (μM)		Acetaldehyde Aqueous Concentration (μM)	
Date	Tape/Pass	Measured	Calculated	Measured	Calculated
05/25/85	434/3	21.9	29.4	5.2	0.058
05/25/85	434/4	31.0	31.9	4.0	0.052
05/26/85	435/2	38.2	81.5	5.8	0.302
05/26/85	435/3	53.6	84.2	4.7	0.43
05/26/85	435/4	42.3	84.6	4.2	0.30
05/27/85	436/2	37.7	62.5	5.2	0.023
05/27/85	436/3	41.7	66.2	7.4	0.023
05/27/85	436/4	46.4	67.2	6.7	0.025
06/10/85	440/3	24.8	48.1	3.9	0.009
06/10/85	440/4	33.6	47.5	7.5	0.012

The comparison of measured and calculated acetaldehyde aqueous concentrations shows a large discrepancy. The calculated values are factors of 10 to 500 smaller than the measured values with an average discrepancy of a factor of 40. This discrepancy could be due to measurement uncertainty or an improper treatment of chemical processes in the model. The same analytical measurement technique was used for the aldehyde collected in the gas phase and in the aqueous phase. Also, the same technique was used for both formaldehyde and acetaldehyde. The technique is aldehyde specific (i.e., no interference with other organic compounds appears likely) and the identification of the aldehydes through the gas chromatograph allows one to identify the various aldehydes. Therefore, it seems that the treatment of acetaldehyde equilibrium chemistry in the model is incorrect. The Henry's law constant has been estimated by different groups and the various values are in close agreement. However, the hydration constant may underestimate the formation of the hydrated form of acetaldehyde. Betterton and Hoffmann (1988) reported an effective Henry's law constant for acetaldehyde of 11.4 M atm^{-1} at 25°C. This value is commensurate with the effective Henry's law constant of 28.6 M atm^{-1} which was used in our simulations. There is, therefore, some question remaining on the difference between the atmospheric measurements reported by Richards (1989) and the laboratory measurements of acetaldehyde solubility.

Section 7
CHEMICAL KINETICS

INTRODUCTION

The evaluation of the performance of a chemical kinetic model requires experimental data in a same air parcel at different times. The integrity of an air parcel will not be conserved over a period of several hours because of transport, dispersion and wind shear phenomena. However, it is possible to follow an air parcel for a few hours and to study its chemistry while taking into account transport and dispersion processes.

Richards et al. (1987) collected cloud chemistry data in air parcels over periods of time ranging from 1 1/2 hours to 3 hours. These data are, therefore, suitable for performance evaluation of the cloud chemistry model. Five case studies were selected: 21 May, 25 May, 26 May, 27 May and 10 June 1985.

Four sets of sampling were performed on 21 May 1985. The initial sampling was performed offshore, the other samplings were performed downwind over the Long Beach and Los Angeles areas. These sampling sets are at 1 hour intervals (sampling times are typically of about 1 hour, the interval between two samplings refers to the interval between the midpoint times of the two samplings). Atmospheric turbulence was reported to be significant on that day.

Three sets of sampling were performed on 25 May 1985, at 44 minute intervals. The initial sampling was performed offshore and the two following samplings were performed over the Long Beach and Los Angeles areas.

Three sets of sampling were performed on 26 May 1985 at 1 hour intervals. These samplings were performed in the Pomona and Ontario areas. Some light rain was reported during the sampling period.

Three sets of sampling were performed on 27 May 1985 at 1 hour intervals. These samplings were also performed in the Pomona and Ontario areas.

Four sets of sampling were performed on 10 June 1985 at intervals ranging from 36 minutes to 54 minutes. The initial sampling was performed offshore. The other samplings were performed over the Long Beach and Los Angeles areas and offshore.

A more detailed description of the sampling, flight patterns and meteorological conditions is presented by Richards et al. (1987).

The model simulations were performed using a single cell with no transport or dispersion. The concentrations measured at the first sampling set were used as initial concentrations for the cloud chemistry model. We discuss next the results of the model evaluation for each one of these five case studies. Then, we discuss the overall results for nitrate and sulfate formation in more detail.

CASE STUDY OF 21 MAY 1985

Table 7-1 presents a comparison of the measured and calculated concentrations of aqueous species for this case study. Measured and calculated concentrations of gaseous species are presented in Table 7-2. Results are not presented for SO_2 because the SO_2 concentrations were below 1 ppb which is less than the measurement uncertainty. Acetaldehyde concentrations are not presented because of the large uncertainty in the equilibrium chemistry of acetaldehyde which was discussed in the previous section.

Concentrations at the initial time present slight differences which are due to round off errors during conversions from ppm to M units for the solute concentrations and to gas/liquid equilibrium calculations for HCHO.

Table 7-1: Comparison of Measured and Calculated Solute Concentrations - Case Study of 21 May 1985

	$SO_4^{2-} + HSO_4^-$	NO_3^-	NH_4^+	$Na^+ + K^+$	$Ca^{2+} + Mg^{2+} + Pb^{2+}$	Cl^-	Fe^{3+}	Mn^{2+}	H_2O_2
Initial Time (0300 LST)									
Measured concentration(M)	2.00×10^{-4}	6.32×10^{-4}	3.83×10^{-4}	3.53×10^{-4}	1.04×10^{-4}	2.91×10^{-4}	8.81×10^{-6}	--	1.63×10^{-4}
Calculated concentration(M)	1.95×10^{-4}	6.17×10^{-4}	3.73×10^{-4}	3.44×10^{-4}	1.02×10^{-4}	2.84×10^{-4}	8.42×10^{-6}	--	1.59×10^{-4}
Calculated/Measured	0.98	0.98	0.97	0.98	0.98	0.98	0.96	-	0.98
60 min.									
Measured concentration(M)	1.58×10^{-4}	4.89×10^{-4}	2.59×10^{-4}	2.03×10^{-4}	4.66×10^{-5} (1)	1.87×10^{-4}	--	--	6.18×10^{-5}
Calculated concentration(M)	2.34×10^{-4}	6.45×10^{-4}	3.86×10^{-4}	3.56×10^{-4}	1.05×10^{-4}	2.87×10^{-4}	8.71×10^{-6}	--	1.57×10^{-4}
Calculated/Measured	1.48	1.32	1.49	1.75	2.25	1.53	--	-	2.54
120 min.									
Measured concentration(M)	3.75×10^{-4}	1.73×10^{-3}	8.57×10^{-4}	4.51×10^{-4}	--	3.34×10^{-4}	--	--	5.32×10^{-5}
Calculated concentration(M)	6.60×10^{-4}	1.83×10^{-3}	1.09×10^{-3}	1.00×10^{-3}	2.97×10^{-4}	7.84×10^{-4}	2.45×10^{-5}	--	3.10×10^{-4}
Calculated/Measured	1.76	1.06	1.27	2.22	-	2.35	--	--	5.83
180 min.									
Measured concentration(M)	2.58×10^{-4}	1.29×10^{-3}	7.68×10^{-4}	3.59×10^{-4}	1.02×10^{-4}	2.26×10^{-4}	1.26×10^{-5}	5.68×10^{-7}	4.44×10^{-5}
Calculated concentration(M)	2.95×10^{-4}	8.27×10^{-4}	4.87×10^{-4}	4.49×10^{-4}	1.33×10^{-4}	3.44×10^{-4}	1.09×10^{-5}	--	1.78×10^{-4}
Calculated/Measured	1.14	0.64	0.63	1.25	1.30	1.52	0.87	-	4.01

(1) Pb^{2+} - not measured

TABLE 7-2 - Comparison of Measured and Calculated Gas Concentrations - Case Study of 21 May 1985

	NO_x	O_3	HCHO
Initial Time (0300 LST)			
Measured concentration (ppb)	0.7	97.1	1.11
Calculated concentration (ppb)	0.7	97.1	0.87
Calculated/Measured	1.00	1.00	0.78
60 min.			
Measured concentration (ppb)	3.10	91.5	1.11
Calculated concentration (ppb)	0.59	97.0	0.88
Calculated/Measured	0.19	1.06	0.79
120 min.			
Measured concentration (ppb)	2.30	84.9	1.11
Calculated concentration (ppb)	0.50	96.9	1.03
Calculated/Measured	0.22	1.14	0.93
180 min.			
Measured concentration (ppb)	3.80	74.2	1.11
Calculated concentration (ppb)	0.43	96.8	0.92
Calculated/Measured	0.11	1.31	0.83

In the model, concentrations of NH_4^+, Na^+, K^+, Ca^{2+}, Mg^{2+}, Pb^{2+}, Fe^{3+} and Mn^{2+} are affected only by variations in the liquid water content since these species do not undergo chemical transformations. Sulfate and nitrate concentrations may increase (for a constant liquid water content) due to chemical formation through oxidation of SO_2 and NO_x, respectively. Chloride concentrations may decrease (for a constant liquid water content) due to reaction with NO_3 radicals in droplets. Concentrations of H_2O_2, O_3 and HCHO may increase or decrease due to chemical reactions. Concentrations of NO_x are likely to decrease due to oxidation to nitrate.

The model calculations show an overprediction of the sulfate concentrations by 14 to 76 percent and an agreement between measured and calculated nitrate concentrations within 40 percent. It should be noted, however, that concentrations of nonreactive ions show differences of as much as a factor of 2. These differences suggest that transport processes were significantly affecting the cloud chemical composition.

The concentration of NO_x increases significantly between the first sampling and the following samplings. This result suggests that NO_x was emitted into or transported from below the cloud as the air parcel moved over the Long Beach and Los Angeles areas. The model calculations show a slight decrease in the NO_x concentration due to oxidation of NO_2 by O_3. However, the low initial NO_x concentration leads to little effect of this chemical pathway on the O_3 concentration. The measurements show a more significant decrease in the O_3 concentration because higher NO_x concentrations are present in the cloud over land.

Only one measurement of HCHO was available. Model calculations show little variation in the HCHO concentration.

CASE STUDY OF 25 MAY 1985

Table 7-3 presents the aqueous concentrations of major species. Comparison of measured and calculated concentrations of the nonreactive ions shows differences of at most 50 percent for NH_4^+ and 35 percent for other ions. This result suggests that transport processes had less effect on cloud chemical composition on 25 May 1985 than on 21 May 1985. This result is consistent with the fact that turbulence was reported to be significantly lower on 25 May 1985 than on 21 May 1985.

The sulfate concentration is underestimated by 24 percent for the second sampling set and overestimated by 35 percent for the third sampling set. The nitrate concentration is underestimated by about 30 percent in both cases.

Table 7-4 shows the calculated and measured gas concentrations. The measured concentrations of NO_x show the same pattern as in the previous case study. The NO_x concentration offshore is about 1 ppb and increases to about 10 ppb over land. This change in NO_x concentration is not present in the model calculation since transport was not considered. It may be noted that the underestimation of nitrate concentrations is likely to be related to the underestimation of NO_x concentrations.

The measured O_3 concentrations show a trend which is consistent with the NO_x concentrations; that is, O_3 concentrations are lower overland than offshore since more NO_x is available to react with O_3 over land. Since calculated NO_x concentrations are low throughout this simulation, the calculated O_3 concentration varies little.

The calculated HCHO concentration shows little variation throughout the simulation.

Table 7-3: Comparison of Measured and Calculated Solute Concentrations - Case Study of 25 May 1985

	$SO_4^{2-} + HSO_4^-$	NO_3^-	NH_4^+	$Na^+ + K^+$	$Ca^{2+}+Mg^{2+}+Pb^{2+}$	Cl^-	Fe^{3+}	Mn^{2+}	H_2O_2
Initial Time (0100 LST)									
Measured concentration (M)	1.80×10^{-4}	3.53×10^{-4}	1.26×10^{-4}	1.42×10^{-4}	3.20×10^{-5}	1.21×10^{-4}	2.48×10^{-6}	1.89×10^{-7}	1.02×10^{-4}
Calculated concentration(M)	1.78×10^{-4}	3.49×10^{-4}	1.25×10^{-4}	1.40×10^{-4}	3.15×10^{-5}	1.20×10^{-4}	2.45×10^{-6}	1.87×10^{-7}	1.02×10^{-4}
Calculated/Measured	0.99	0.99	0.99	0.99	0.98	0.99	0.99	0.99	1.00
44 min.									
Measured concentration(M)	1.68×10^{-4}	3.81×10^{-4}	1.57×10^{-4}	1.34×10^{-4}	3.05×10^{-5}	1.18×10^{-4}	2.22×10^{-6}	1.28×10^{-7}	3.89×10^{-5}
Calculated concentration(M)	1.28×10^{-4}	2.42×10^{-4}	8.53×10^{-5}	9.56×10^{-5}	2.15×10^{-5}	7.83×10^{-5}	1.67×10^{-6}	1.27×10^{-7}	7.13×10^{-5}
Calculated/Measured	0.76	0.64	0.54	0.71	0.71	0.66	0.75	0.99	1.83
88 min.									
Measured concentration(M)	1.23×10^{-4}	4.58×10^{-4}	1.90×10^{-4}	9.24×10^{-5}	2.73×10^{-5}	6.34×10^{-5}	2.47×10^{-6}	1.48×10^{-7}	4.97×10^{5}
Calculated concentration(M)	1.66×10^{-4}	3.17×10^{-4}	1.10×10^{-4}	1.23×10^{-4}	2.77×10^{-5}	9.67×10^{-5}	2.16×10^{-6}	1.64×10^{-7}	8.54×10^{-5}
Calculated/Measured	1.35	0.69	0.58	1.33	1.02	1.53	0.87	1.11	1.72

TABLE 7-4 - Comparison of Measured and Calculated Gas Concentrations - Case Study of 25 May 1985

	NO_x	O_3	HCHO
Initial Time (0100 LST)			
Measured concentration (ppb)	1.10	80.4	2.10
Calculated concentration (ppb)	1.10	80.4	1.56
Calculated/Measured	1.00	1.00	0.74
44 min.			
Measured concentration (ppb)	9.20	61.6	2.10
Calculated concentration (ppb)	0.99	80.3	1.43
Calculated/Measured	0.11	1.30	0.68
88 min.			
Measured concentration (ppb)	10.40	66.0	2.10
Calculated concentration (ppb)	0.89	80.1	1.55
Calculated/Measured	0.09	1.21	0.74

CASE STUDY OF 26 MAY 1985

Table 7-5 shows the calculated and measured aqueous concentrations. Comparison of measured and calculated concentrations of nonreactive species shows a increasing trend toward overprediction by about a factor of 2 after 1 hour and by about a factor of 4 to 5 after 2 hours. This result is consistent with the fact that light rain on that day may have depleted the concentrations of ions in cloud droplets.

Concentrations of sulfate and nitrate show good agreement between measured and calculated values after 1 hour but are overestimated by about a factor of 2 after 2 hours. This result suggests that sulfate and nitrate were removed by rain but were also formed or transported upward into the cloud, therefore, their concentrations show less decrease than those of the nonreactive species.

The calculated H_2O_2 aqueous concentrations show very good agreement with the measured values.

Gas concentrations are presented in Table 7-6. The concentration of NO_x varies little over the two hour period and shows a slight decrease both in the measurements and simulation results. The O_3 concentration shows little variation and the calculated values are in excellent agreement with the measured values.

The HCHO concentration shows little variation over the two-hour simulation.

CASE STUDY OF 27 MAY 1985

Aqueous concentrations are presented in Table 7-7. Comparison of calculated and measured concentrations of nonreactive ions shows an overprediction by about a factor of two after 1 hour and a slight underprediction by 10 to 40 percent after 2 hours. This result probably reflects variations due to transport and dispersion phenomena.

Table 7-5: Comparison of Measured and Calculated Solute Concentrations - Cast Study of 26 May 1985

	$SO_4^{2-} + HSO_4^-$	NO_3^-	NH_4^+	$Na^+ + K^+$	$Ca^{2+} + Mg^{2+} + Pb^{2+}$	Cl^-	Fe^{3+}	Mn^{2+}	H_2O_2
Initial Time (0034 LST)									
Measured concentration(M)	1.52×10^{-4}	5.94×10^{-4}	3.26×10^{-4}	1.39×10^{-4}	5.42×10^{-5}	9.14×10^{-5}	5.73×10^{-6}	3.08×10^{-7}	3.03×10^{-5}
Calculated concentration(M)	1.52×10^{-4}	5.88×10^{-4}	3.23×10^{-4}	1.38×10^{-4}	5.36×10^{-5}	9.08×10^{-5}	5.59×10^{-6}	3.06×10^{-7}	3.06×10^{-5}
Calculated/Measured	1.00	0.99	0.99	0.99	0.99	0.99	0.98	0.99	1.01
60 min.									
Measured concentration(M)	1.35×10^{-4}	5.43×10^{-4}	2.70×10^{-4}	7.68×10^{-5}	2.82×10^{-5}	6.75×10^{-5}	2.39×10^{-6}	1.40×10^{-7}	2.52×10^{-5}
Calculated concentration(M)	1.49×10^{-4}	5.12×10^{-4}	2.70×10^{-4}	1.15×10^{-4}	4.47×10^{-5}	5.57×10^{-5}	4.66×10^{-6}	2.55×10^{-7}	2.50×10^{-5}
Calculated/Measured	1.11	0.94	1.00	1.50	1.59	0.83	1.95	1.82	0.99
120 min.									
Measured concentration(M)	1.02×10^{-4}	4.41×10^{-4}	4.61×10^{-4}	4.07×10^{-5}	1.54×10^{-5}	4.86×10^{-5}	1.13×10^{-6}	6.94×10^{-8}	2.88×10^{-5}
Calculated concentration(M)	2.03×10^{-4}	7.09×10^{-4}	3.60×10^{-4}	1.53×10^{-4}	5.96×10^{-5}	5.03×10^{-5}	6.21×10^{-6}	3.40×10^{-7}	3.06×10^{-5}
Calculated/Measured	1.99	1.61	0.78	3.76	3.87	1.03	5.50	4.90	1.06

TABLE 7-6 - Comparison of Measured and Calculated Gas Concentrations - Case Study of 26 May 1985

	NO_x	O_3	HCHO
Initial Time (0034 LST)			
Measured concentration (ppb)	7.10	57.7	5.98
Calculated concentration (ppb)	7.10	57.7	4.82
Calculated/Measured	1.00	1.00	0.81
60 min.			
Measured concentration (ppb)	7.50	58.3	5.98
Calculated concentration (ppb)	6.44	57.0	4.54
Calculated/Measured	0.86	0.98	0.76
120 min.			
Measured concentration (ppb)	6.40	57.9	5.98
Calculated concentration (ppb)	5.85	56.4	4.97
Calculated/Measured	0.91	0.97	0.83

Table 7-7: Comparison of Measured and Calculated Solute Concentrations - Case Study of 27 May 1985

	$SO_4^{2-} + HSO_4^-$	NO_3^-	NH_4^+	$Na^+ + K^+$	$Ca^{2+} + Mg^{2+} + Pb^{2+}$	Cl^-	Fe^{3+}	Mn^{2+}	H_2O_2
Initial Time (0137 LST)									
Measured concentration(M)	1.52×10^{-4}	7.15×10^{-4}	4.32×10^{-4}	1.53×10^{-4}	5.32×10^{-5}	1.01×10^{-4}	4.88×10^{-6}	3.19×10^{-7}	4.01×10^{-5}
Calculated concentration(M)	1.52×10^{-4}	7.16×10^{-4}	4.32×10^{-4}	1.53×10^{-4}	5.32×10^{-5}	1.01×10^{-4}	4.76×10^{-6}	3.21×10^{-7}	4.06×10^{-5}
Calculated/Measured	1.00	1.00	1.00	1.00	1.00	1.00	0.98	1.01	1.01
60 min.									
Measured concentration(M)	1.67×10^{-4}	9.57×10^{-4}	4.50×10^{-4}	1.14×10^{-4}	5.38×10^{-5} (1)	9.59×10^{-5}	5.97×10^{-6}	3.22×10^{-7}	4.31×10^{-5}
Calculated concentration(M)	2.23×10^{-4}	1.11×10^{-3}	6.35×10^{-4}	2.24×10^{-4}	7.81×10^{-5}	9.50×10^{-5}	6.98×10^{-6}	4.70×10^{-7}	5.17×10^{-5}
Calculated/Measured	1.34	1.16	1.41	1.96	1.45	0.99	1.17	1.46	1.20
120 min.									
Measured concentration(M)	1.79×10^{-4}	1.03×10^{-3}	8.73×10^{-4}	1.95×10^{-4}	8.20×10^{-5}	1.07×10^{-4}	8.46×10^{-6}	4.35×10^{-7}	5.70×10^{-5}
Calculated concentration(M)	1.85×10^{-4}	9.72×10^{-4}	5.29×10^{-4}	1.87×10^{-4}	6.51×10^{-5}	3.85×10^{-5}	5.82×10^{-6}	3.92×10^{-7}	4.42×10^{-5}
Calculated/Measured	1.03	0.94	0.61	0.96	0.79	0.36	0.69	0.90	0.78

(1) Pb^{++} not measured.

The concentration of sulfate is overpredicted by about 30 percent and shows close agreement between measured and calculated values after 2 hours.

The concentrations of nitrate and H_2O_2 show good agreement between measured and calculated values (i.e., within about 20 percent).

The concentration of chloride shows a significant underprediction which results from the model reaction of NO_3 radicals with chloride ions. Calculated and measured gas concentrations are shown in Table 7-8. The measured NO_x concentration shows some variation between 5 and 6 ppb whereas the model calculation shows a steady decrease of the NO_x concentration which amounts to about 1 ppb after 2 hours.

The measured O_3 concentration varies within about 3 ppb (i.e., about 5 percent of the initial concentration) while the calculated O_3 concentration shows a decrease that parallels that of NO_x.

The HCHO concentration shows little variation over the two-hour simulation.

CASE STUDY OF 10 JUNE 1985

Calculated and measured aqueous concentrations are presented in Table 7-9. Comparison of calculated and measured nonreactive ion concentrations shows underprediction after 36 and 72 minutes and reasonable agreement after 126 minutes. The underprediction probably results from vertical entrainment of air from below the cloud as the air parcel moves over land. The last sampling set was performed offshore, which may explain the better agreement between measured and calculated values.

TABLE 7-8 - Comparison of Measured and Calculated Gas Concentrations - Case Study of 27 May 1985

	NO_x	O_3	HCHO
Initial Time (0137 LST)			
Measured concentration (ppb)	5.30	56.9	3.56
Calculated concentration (ppb)	5.30	56.9	3.26
Calculated/Measured	1.00	1.00	0.92
60 min.			
Measured concentration (ppb)	6.00	57.1	3.56
Calculated concentration (ppb)	4.84	56.4	3.47
Calculated/Measured	0.81	0.99	0.97
120 min.			
Measured concentration (ppb)	5.80	53.9	3.56
Calculated concentration (ppb)	4.43	56.0	3.38
Calculated/Measured	0.76	1.04	0.95

Table 7-9: Comparison of Measured and Calculated Solute Concentrations - Case Study of 10 June 1985

	$SO_4^{2-} + HSO_4^-$	NO_3^-	NH_4^+	$Na^+ + K^+$	$Ca^{2+} + Mg^{2+} + Pb^{2+}$	Cl^-	Fe^{3+}	Mn^{2+}	H_2O_2
Initial Time (0148 LST)									
Measured concentration(M)	7.12×10^{-5}	1.40×10^{-4}	6.30×10^{-5}	1.18×10^{-4}	3.20×10^{-5}	1.02×10^{-4}	1.49×10^{-6}	1.18×10^{-7}	8.14×10^{-5}
Calculated concentration(M)	7.10×10^{-5}	1.39×10^{-4}	6.28×10^{-5}	1.17×10^{-4}	3.21×10^{-5}	1.02×10^{-4}	1.43×10^{-6}	1.19×10^{-7}	8.14×10^{-5}
Calculated/Measured	1.00	0.99	1.00	0.99	1.00	1.00	0.96	1.01	1.00
36 min.									
Measured concentration(M)	3.33×10^{-4}	5.97×10^{-4}	3.46×10^{-4}	5.87×10^{-4}	3.83×10^{-4}	4.87×10^{-4}	5.97×10^{-6}	--	--
Calculated concentration(M)	1.42×10^{-4}	3.79×10^{-4}	1.25×10^{-4}	2.35×10^{-4}	6.42×10^{-5}	1.17×10^{-4}	2.85×10^{-6}	2.37×10^{-7}	1.24×10^{-4}
Calculated/Measured	0.43	0.63	0.36	0.40	1.68	0.24	0.48	--	--
72 min.									
Measured concentration(M)	2.68×10^{-4}	6.98×10^{-4}	4.93×10^{-4}	3.42×10^{-4}	8.28×10^{-5}	2.38×10^{-4}	7.16×10^{-6}	4.55×10^{-7}	7.21×10^{-5}
Calculated concentration(M)	1.07×10^{-4}	3.56×10^{-4}	9.40×10^{-5}	1.76×10^{-4}	4.81×10^{-5}	2.48×10^{-5}	2.14×10^{-6}	1.78×10^{-7}	1.01×10^{-4}
Calculated/Measured	0.40	0.51	0.19	0.51	0.58	0.10	0.30	0.39	1.40
126 min.									
Measured concentration(M)	1.28×10^{-4}	2.85×10^{-4}	1.02×10^{-4}	2.13×10^{-4}	4.70×10^{-5}	5.16×10^{-4}	2.98×10^{-6}	1.58×10^{-7}	9.71×10^{-5}
Calculated concentration(M)	1.31×10^{-4}	6.23×10^{-4}	1.16×10^{-4}	2.16×10^{-4}	5.92×10^{-5}	1.0×10^{-20}	2.85×10^{-6}	2.37×10^{-7}	6.95×10^{-5}
Calculated/Measured	1.02	2.19	1.14	1.01	1.26	1.94×10^{-17}	0.96	1.50	0.72

(1) Pb^{++} not measured

The sulfate concentrations show the same pattern which suggest that sulfate concentrations are primarily governed by transport phenomena. The nitrate concentrations also show underprediction after 36 and 72 minutes, but show an overprediction by a factor of two after 126 minutes which must result from an overprediction of nitrate formation or underprediction of dispersion.

The chloride concentration shows a large underprediction as the model chloride concentrations are totally depleted by reaction with NO_3 radicals.

Gas concentrations are presented in Table 7-10. The measured NO_x concentration increases from about 10 ppb to 13 ppb as the air parcel moves over land. The measured O_3 concentration decreases by about 16 ppb as the air parcel moves from offshore toward the land.

The calculated NO_x concentration decreases by about 2 ppb during the two hours while a larger decrease of 6 ppb is calculated for the O_3 concentration.

NITRATE CHEMISTRY

The chemistry of nitrate formation was studied in detail for each one of the five case studies. To that end, the measured nitrate concentrations were scaled so that the corresponding Na^+, K^+, Mg^{2+} and Ca^{2+} concentrations remained constant on average. These four cations represent nonreactive species and this procedure allows one to study the variations of nitrate concentrations due to chemical processes by minimizing the variations due to transport phenomena.

The formation of nitrate can be expressed either as the relative increase in nitrate concentration with respect to the initial concentration (i.e., as the ratio of the nitrate concentration at a

TABLE 7-10 - Comparison of Measured and Calculated Gas Concentrations - Case Study of 10 June 1985

	NO_x	O_3	HCHO
Initial Time (0148 LST)			
Measured concentration (ppb)	9.70	68.3	3.52
Calculated concentration (ppb)	9.70	68.3	2.87
Calculated/Measured	1.00	1.00	0.82
36 min.			
Measured concentration (ppb)	13.80	52.3	3.52
Calculated concentration (ppb)	8.99	64.1	3.18
Calculated/Measured	0.65	1.23	0.90
72 min.			
Measured concentration (ppb)	13.70	50.1	3.52
Calculated concentration (ppb)	8.34	63.4	3.09
Calculated/Measured	0.61	1.27	0.88
126 min.			
Measured concentration (ppb)	13.40	60.0	3.52
Calculated concentration (ppb)	7.45	62.5	3.17
Calculated/Measured	0.56	1.04	0.90

given time to the initial nitrate concentration) or as the absolute amount of nitrate formed. Table 7-11 presents a comparison of these measured and calculated increases in nitrate concentrations. Changes in the measured nitrate concentrations generally exceed the aqueous measurement uncertainty and are, therefore, significant.

It appears that on 21, 25 and 26 May 1985, nitrate formation is significantly underpredicted by the model. For the first two case studies, this underprediction is due in part to the fact that the initial NO_x concentration is not representative of NO_x concentrations at later times since NO_x is entrained into the cloud as the air parcel moves over land.

Therefore, the amount of NO_x available for nitrate formation is significantly underestimated in a model simulation which does not consider transport processes.

On 26 May 1985, the NO_x initial concentration is commensurate with the NO_x concentration at later times. Therefore, either there is transport of nitrate from below the cloud less rainout of nitrate compared to inert species or the model underestimates the chemical conversion of NO_x to nitrate for this case study.

The simulations of 27 May and 10 June 1985 show increases in calculated nitrate concentrations which are consistent with the measurements. For the 27 May 1985 simulation, the nitrate concentration increases by about 1 ppb (10 percent) over the two hours of simulation, whereas the measurements show an increase of 4 ppb (50 percent) after one hour but a similar decrease during the following hour. For the simulation of 10 June 1985, the nitrate concentration increases by 3 ppb (140 percent) over about 2 hours. The measurements show a maximum increase of 2 ppb (90 percent) after about 1 hour.

Table 7-12 presents an assessment of the major chemical pathways that lead to nitrate formation for the five case studies. The two predominant pathways are (1) the formation of NO_3 radicals in the

Table 7-11: Comparison of Measured and Calculated Nitrate Formation

Date	Simulation Time (min)	Factor of Increase in Nitrate Concentration[1]		Increase in Nitrate Concentration (ppb)	
		Measurements	Simulations	Measurements	Simulations
05/21/85	60	1.55	1.01	5.5	0.1
	120	1.91	1.02	9.1	0.2
	180	2.03	1.03	10.4	0.3
05/25/85	44	1.16	1.02	1.2	0.15
	88	1.46	1.03	3.4	0.22
05/26/85	60	1.87	1.04	13.9	0.64
	120	2.86	1.09	29.7	1.44
05/27/85	60	1.49	1.06	4.2	0.52
	120	1.02	1.11	0.2	0.95
06/10/85	36	1.12	1.36	0.25	0.75
	72	1.86	1.70	1.81	1.50
	126	1.34	2.40	0.72	2.95

(1) The factor of increase is defined as the nitrate concentration at a given time divided by the nitrate concentration at the initial time. For the measured values, nitrate concentrations normalized to the Na^+, K^+, Mg^{2+} and Ca^{2+} concentrations were used.

Table 7-12: Contribution of Major Chemical Pathways to Nitrate Formation

Date	Initial NO_x Concentration (ppb)	Initial Nitrate Concentration (ppb)	Nitrate Formed (ppb)	Relative Contributions of Major Pathways (%) $NO_3(aq)$	N_2O_5
21 May 1985	0.7	10.0	0.3	98	2
25 May 1985	1.1	7.5	0.2	97	3
26 May 1985	7.1	16.0	1.4	85	15
27 May 1985	5.3	8.6	1.0	81	19
10 June 1985	9.7	2.1	3.0	77	23

gas-phase, their dissolution in droplets, and their reaction with ions such as chloride ion to form nitrate and (2) the heterogeneous hydrolysis of N_2O_5 at the surface of droplets. These results are consistent with the fact that at night the formation of nitrate tends to take place through the NO_3 chemistry rather than through the OH chemistry (Richards, 1983, Gautier et al., 1985, Seigneur, 1987). Exceptions are nighttime conditions near ground level and plumes aloft where NO concentrations are high and exceed O_3 levels (Seigneur and Saxena, 1984, Killus and Whitten, 1985, Seigneur et al., 1985); then, OH levels may be high enough despite the lack of photochemical activity.

It is interesting to note that the N_2O_5 pathway becomes more important as the NO_x concentration increases. This result is due to the fact that the formation of N_2O_5 is indirectly second-order in NO_2. Therefore, as the NO_2 concentration increases the N_2O_5 concentration will increase proportionally to the square of the NO_2 concentration whereas the NO_3(aq) concentration increases linearly with the NO_2 concentration.

SULFATE CHEMISTRY

The chemistry of sulfate formation was investigated in detail for each one of the five case studies. However, because the measured SO_2 concentrations were below 1 ppb which is less than the measurement uncertainty, the comparison between measured and calculated values cannot provide a true model performance evaluation.

Table 7-13 presents a comparison of measured and calculated increases in sulfate concentrations. In all case studies, the calculated sulfate formation corresponded to the initial SO_2 concentration, i.e., all SO_2 was oxidized to sulfate over the simulation period. This result is due to the fact that the initial SO_2 concentrations are very low and SO_2 is rapidly titrated by H_2O_2 and may react with other oxidants as well. In two cases, 27 May and 10 June 1985, the initial SO_2 concentration was zero and no sulfate was formed.

Table 7-13: Comparison of Measured and Calculated Sulfate Formation

Date	Simulation Time (min)	Factor of Increase in Sulfate Concentration[1]		Increase in Sulfate Concentration (ppb)	
		Measurements	Simulations	Measurements	Simulations
05/21/85	60	1.58	1.16	0.8	0.5
	120	1.49	1.16	1.5	0.5
	180	1.28	1.16	0.9	0.5
05/25/85	44	1.00	1.05	0.0	0.2
	88	0.77	1.06	-0.9	0.2
05/26/85	60	1.81	1.19	3.3	0.8
	120	2.59	1.21	6.5	0.9
05/27/85	60	1.23	1.00	0.4	0
	120	0.85	1.00	-0.3	0
06-10/85	36	1.22	1.00	0.2	0
	72	1.40	1.00	0.4	0
	126	1.18	1.00	0.2	0

(1) The factor of increase is defined as the sulfate concentration at a given time divided by the sulfate concentration at the initial time. For the measured values, sulfate concentrations normalized to the Na^+, K^+, Mg^{2+} and Ca^{2+} concentrations were used.

Measured increases in sulfate concentrations are less than 1.5 ppb on 21, 25, 27 May and 10 June 1985. Decreases are observed on two occasions. Therefore, these variations may be due to measurement uncertainties and to atmospheric transport and dispersion rather than to chemical reactions. On 26 May 1985 the measured increase in sulfate concentration reached 6.5 ppb. This increase parallels the large increase in nitrate concentration and may be due to a significant vertical transport from below the cloud or to less rainout of sulfate compared to inert species.

The contribution of major chemical pathways to sulfate formation is summarized in Table 7-14. It appears that aqueous oxidation of SO_2 by H_2O_2 is the major chemical pathway for sulfate formation. For the case study of 26 May 1985, catalyzed oxidation of SO_2 by O_2 and aqueous oxidation of SO_2 by OH radicals also contribute noticeably to sulfate formation.

Table 7-14: Contribution of Major Chemical Pathways to Sulfate Formation

Date	Initial SO_2 Concentration (ppb)	Initial Sulfate Concentration (ppb)	Sulfate formed (ppb)	Relative Contributions of Major Pathways (%)		
				H_2O_2 (aq)	O_2 (aq)	OH (aq)
21 May 1985	0.5	3.1	0.5	99	<1	<1
25 May 1985	0.2	3.8	0.2	99	<1	<1
26 May 1985	0.9	4.1	0.9	93	5	2
27 May 1985	0	1.8	0	--	-	--
10 June 1985	0	1.1	0	--	-	--

Section 8
CHEMICAL KINETICS AND TRANSPORT

INTRODUCTION

It appeared from the results of the chemical kinetics simulations that were presented in Section 7 that the changes in sulfate and nitrate concentrations could not be solely explained with chemical kinetics and implied that vertical transport probably played a significant role in governing cloud species concentrations. Richards et al. (1987) also suggested that vertical transport was important based on the variation of inert species concentrations such as lead and ammonium. Therefore, it is necessary to consider vertical transport if one wants to provide a realistic description of the evolution of cloud species concentrations. In this section, we present the results of two simulations conducted with cloud chemistry and vertical transport.

Two case studies were selected to analyze the cloud chemistry and vertical transport processes. These two case studies are those of 25 May and 26 May 1985. If one considers the nitrate and sulfate concentrations normalized with respect to chemically inert ion concentrations, there was some significant increase in nitrate concentrations with time on both of these days; on 26 May, there was also a clear trend toward increasing sulfate concentrations. On 27 May and 10 June 1985, nitrate and sulfate concentrations varied without any particular trend. On 21 May 1985, nitrate concentrations increased steadily with time; however, turbulence was high on that day which may complicate the simulation of transport processes. No rain was observed on 25 May, a little drizzle was observed on 26 May.

The flight of 25 May 1985 represents an air parcel trajectory that starts offshore and moves inland over Long Beach and Los Angeles. The total period of simulation in 88 min. The flight of 26 May 1985 represents an air parcel trajectory that starts above Pomona and moves eastward toward Ontario.

INPUT DATA

The input data for these simulations were prepared as follows. In the cloud layer, input data were similar to those presented in Section 7.

Temperature, relative humidity and liquid water content vertical profiles were available from the aircraft spirals and missed instrument landing approaches. Aircraft data also provided concentrations of NO, NO_2, O_3, and SO_2. No vertical profile data were available for hydrocarbons, aerosols, HNO_3, NH_3, and H_2O_2. No direct data were available on vertical transport variables such as updraft velocity and vertical diffusion coefficient.

Concentrations of hydrocarbons were assumed to be proportional to NO_x concentrations since automobiles are a major common source of these compounds. Concentrations of primary aerosols (sodium, potassium, magnesium, calcium, iron, manganese and lead) were assumed to be constant with height since these species are unreactive and no information on their vertical profile was available. The concentration of H_2O_2 was also assumed to be constant with height; the below-cloud H_2O_2 should be unreactive and its concentration should not therefore be less than the cloud H_2O_2 concentration.

Concentrations of sulfate, nitrate (HNO_3 and aerosol nitrate) and ammonium/ammonia below the clouds were estimated as follows. For 25 May 1985, 24-hour average concentrations of sulfate and nitrate

PM-10 aerosols were available (ARB, 1987). These concentrations were assumed to be twice as much for 26 May 1985 since the measured aerosol scattering coefficient was about twice as much on 26 as on 25 May. The nighttime concentrations of sulfate and nitrate were estimated based on diurnal profiles reported by Grosjean (1988) for nitrate aerosol and by John et al. (1985) for sulfate aerosol. The nitric acid and ammonia concentrations were estimated based on the data of Russell and Cass (1984). The ammonium aerosol concentrations were estimated based on the thermodynamic analysis of Pilinis and Seinfeld (1987) for sodium and ammonium salts of sulfate and nitrate aerosols. The chloride aerosol concentration was calculated to provide electroneutrality between sulfate, nitrate, ammonium, sodium, magnesium, calcium, potasium, lead, iron and manganese.

Concentrations of major species below and in the cloud at the beginning of the model simulations are presented in Tables 8-1 and 8-2 for the 25 May and 26 May 1985 simulations, respectively.

The vertical profile of the liquid water content was available from the aircraft forward scattering spectroscopic probe (FSSP). However, the King probe data were assumed to be more reliable and were used in the cloud simulations presented in Sections 6 and 7. Consequently, the FSSP data were scaled to the King probe data to obtain the liquid water contents as function of height.

The vertical diffusion coefficient was assumed to be 20 m^2/s, a typical value for stratus clouds.

The updraft velocity was not measured; it is, however, a critical parameter since it defines the rate of upward transport of pollutants from below the cloud into the cloud. The updraft velocity was estimated by means of a cloud physics model based on the formulation of Kessler (1969). The inputs to this cloud physics

Table 8-1. Initial Concentrations of Major Chemical Species below and in the Cloud; Simulation of 25 May 1985

Species	Below-Cloud	In-Cloud
NO (ppb)	0	0
NO_2 (ppb)	12.0	1.1
O_3 (ppb)	68.0	80.0
SO_2 (ppb)	0	0.2
Sulfate (ppb)	1.3	3.8
Nitrate (ppb)	1.9	7.4
Ammonium (ppb)	5.7	2.6

Table 8-2. Initial Concentrations of Major Chemical Species below and in the Cloud; Simulation of 26 May 1985

Species	Below-Cloud	In-Cloud
NO (ppb)	0	0
NO_2 (ppb)	8.0	7.1
O_3 (ppb)	45.0	57.7
SO_2 (ppb)	1.0	0.9
Sulfate (ppb)	2.6	4.1
Nitrate (ppb)	3.8	15.8
Ammonium (ppb)	12.0	8.7

model are the updraft velocity, the vertical temperature and pressure profiles, and the relative humidity below the cloud. The outputs of the model include the liquid water content of the cloud and precipitation rate. The cloud model was used with a variety of updraft velocities to determine which updraft velocity led to a cloud water content and a precipitation rate that corresponded to the observations. Updraft velocities of 0.065 and 0.077 m/s were selected in this manner for the 25 May and 26 May 1985 simulations, respectively.

No precipitation occured on 25 May 1985 but a light drizzle occured on 26 May 1985. We assumed that species present in coarse aerosols such as sodium, potasium, calcium, magnesium, iron, manganese, lead and chloride were totally present in the droplet phase; i.e. the scavenging efficiency of the rain was 1. For sulfate, nitrate and ammonium aerosols which are present mostly in the submicron range, we assumed that the scavenging efficiency of rain drops was 0.1. This assumption is based on the fact that submicron aerosols are not scavenged efficiently by rain drops (e.g., Seigneur and Barnes, 1986).

SIMULATION OF 25 MAY 1985

The results of the simulation of 25 May 1985 are presented in Table 8-3 for the concentrations of major species. It appears that calculated concentrations of sulfate and nitrate decrease steadily because concentrations of these species are lower below cloud than in the cloud at the initial time, and chemical formation of these species is not sufficient to compensate for the decrease in concentration due to vertical transport. The measured sulfate concentration first increases, then decreases below its initial value. The measured nitrate concentration shows a significant increase after 44 min, then, remains about constant for the next

Table 8-3. Comparison of Measured and Calculated Cloud Concentrations of Major Chemical Species. Simulation of 25 May 1985

	Simulation Time (min)		
	0	44	88
Sulfate (ppb)			
Measured	3.76	5.15	3.01
Calculated	3.76	3.34	2.55
Nitrate (ppb)			
Measured	7.37	11.70	11.20
Calculated	7.37	6.36	5.92
Ammonium (ppb)			
Measured	2.64	4.82	4.63
Calculated	2.64	3.35	4.24
pH			
Measured	3.26	3.33	3.36
Calculated	3.31	3.60	3.74
NO_2 (ppb)			
Measured	1.1	9.2	10.4
Calculated	1.1	3.2	5.2
O_3 (ppb)			
Measured	80.4	61.6	66.0
Calculated	80.4	77.0	72.2

44 min. This increase is significant since it exceeds the measurement uncertainty. It cannot be explained with our present knowledge of nitrate chemistry and is not consistent with the lower below-cloud concentrations assumed for this simulation.

The calculated and measured ammonium concentrations are in reasonable agreement with an increase that results from the entrainment of higher ammonium concentrations from below the cloud into the cloud.

The measured pH shows a slight increase whereas the calculated pH shows a more significant increase due to the decrease in sulfate and nitrate concentrations.

The concentration of NO_2 increases in both the simulation and the measurements. However, the increase is significantly less in the simulation than in the measurements and the difference between measured and calculated values exceeds the measurement uncertainty. This result suggests that the actual NO_x concentrations transported into the cloud were greater than in the simulation. Emission of NO_x from tall stacks located along the coast were not considered in our simulation and may be the cause of the discrepancy between measured and calculated NO_x concentrations. The O_3 concentration follows a pattern related to that of NO_2. Concentrations of NO_2 inland are much higher than offshore due to NO and NO_2 emissions from automobiles and other sources; conversely, O_3 concentrations are lower inland due to reaction with NO emissions. Therefore, O_3 concentrations are lower below-cloud than in-cloud and O_3 concentrations decrease in the cloud as the updraft entrains lower O_3 concentrations into the cloud. Richards et al. (1987) reported that O_3 concentrations along a flight orbit were higher outside of clouds than inside clouds. Seigneur and Saxena (1985) simulated the effect of clouds on O_3 chemistry and their results showed that O_3 concentrations

are not significantly affected by cloud chemistry. Therefore, the variations observed by Richards el al. (1987) in O_3 concentrations inside and outside of clouds must correspond to the sampling of different air parcels.

The comparison of measured and calculated concentrations with transport and chemistry show some discrepancies which suggest that (1) emissions from tall stacks into elevated cloud layers may contribute significantly to NO_x concentrations in coastal clouds and (2) the below-cloud concentrations of sulfate and nitrate may not have been estimated accurately and actual measurements would be necessary for further model evaluation.

SIMULATION OF 26 MAY 1985

The results of the simulation of 26 May 1985 are presented in Table 8-4 for the concentrations of major species.

There is good agreement between the measured and calculated sulfate concentrations with a slight decrease over the two-hour period. The nitrate concentrations also show a decrease over the two-hour period although the decrease is larger in the calculated concentrations than in the measured concentrations. The decreases in measured concentrations exceed the measurement uncertainties and can therefore be considered as significant changes in the measured concentrations.

The largest discrepancy between measured and calculated concentrations appear for the ammonium concentrations. The simulation shows first an increase due to the entrainment of higher concentrations from below the cloud, then, a decrease due to the rainout of ammonium. The measured values show an increase in ammonium concentration over the two-hour period.

Table 8-4. Comparison of Measured and Calculated Cloud Concentrations of Major Chemical Species. Simulation of 26 May 1985

	Simulation Time (min)		
	0	60	120
Sulfate (ppb)			
Measured	4.06	4.35	2.47
Calculated	4.06	3.61	2.53
Nitrate (ppb)			
Measured	15.80	17.50	10.70
Calculated	15.80	10.75	7.00
Ammonium (ppb)			
Measured	8.68	8.72	11.20
Calculated	8.68	8.92	7.06
pH			
Measured	3.35	3.31	3.65
Calculated	3.40	3.61	3.73
NO_2 (ppb)			
Measured	7.10	7.50	6.40
Calculated	7.10	6.59	6.00
O_3 (ppb)			
Measured	57.7	58.3	57.9
Calculated	57.7	53.5	51.0

The pH increases in both the calculations and the measurements. The increase in pH are quite commensurate: 0.30 in the measurements and 0.33 in the simulation.

The concentration of NO_2 shows a slight decrease in both measurements and calculations, which results from the conversion of NO_2^- to nitrate. The decrease in the measurements is, however, within the measurement uncertainty.

The calculated O_3 concentration decreases as lower O_3 concentrations are entrained from below the cloud. Little variation appears in the measured O_3 concentrations.

The concentrations of inert species such as sodium, potassium, calcium, magnesium, iron and manganese decreased, on average, by 43 and 78 percent from the initial concentrations after 1 and 2 hours, respectively. The calculated decreases in these concentrations were 63 and 82 percent after 1 and 2 hours, respectively. This good agreement between measured and calculated inert species concentrations suggests that the major vertical transport processes (updraft and rain) are treated satisfactorily in this simulation.

Overall, there is good agreement between the results of the model simulation of transport and chemistry for the case study of 26 May 1985 and the measured values of cloud species concentrations. Consequently, this case study was selected for further analysis of the physical and chemical processes that affect acid formation in clouds.

Section 9
SENSITIVITY ANALYSIS STUDIES

INTRODUCTION

The simulation of the atmospheric physical and chemical processes of air pollution is particularly useful to investigate the relative importance of these processes which govern air pollution levels and the effect in changes in precursor levels on air pollution levels. The study of the physical and chemical processes that govern the formation of air pollutants allows one to determine the parameters to which the model is the most sensitive and, therefore, which parameters need to be known with accuracy to obtain satisfactory model performance. The effect of changes in precursor levels on air pollution levels provides some useful information for the development of air pollution control strategies.

Because satisfactory model performance was obtained for the simulation of 26 May 1985, we used this simulation as the base case for these sensitivity analysis studies. Nineteen sensitivity study simulations were performed. Eight simulations pertain to changes in precursor levels. Six simulations address the sensitivity of the model to physical and chemical parameters. Five simulations consider the effect of different environmental conditions on the model simulation results. These simulations are summarized in Table 9-1.

SENSITIVITY TO PRECURSOR LEVELS

A key issue in the chemistry of atmospheric acidity is the response of the concentration of major chemical species to the concentrations of precursors. Previous work has demonstrated that the responses of sulfate to SO_2, nitrate to NO_x, and sulfate and nitrate to

Table 9-1. Sensitivity Studies Performed with the Simulation of 26 May 1985

Simulation Number	Description of Sensitivity Study
1	SO_2 initial concentrations equal to 0 ppb
2	SO_2 initial concentrations equal to 0.5 ppb
3	SO_2 initial concentrations equal to 1 ppb
4	SO_2 initial concentrations equal to 2 ppb
5	SO_2 initial concentrations equal to 4 ppb
6	NO_x initial concentrations divided by 2
7	RHC initial concentrations divided by 2
8	NH_3 initial concentrations divided by 2
9	Kinetics of N_2O_5 heterogeneous hydrolysis assumed to be limited by N_2O_5 diffusion only
10	Accommodation coefficient of NO_3 equal to 1
11	Accommodation coefficient of NO_3 equal to 0.01
12	Accommodation coefficient of NO_3 equal to 10^{-6}
13	Updraft velocity multiplied by 2
14	Liquid water content multiplied by 2
15	Daytime cloud simulation
16	Non-raining cloud simulation
17	Cloud free simulation
18	Ground-level fog simulation
19	Plume/cloud simulation

hydrocarbon concentrations can be highly non-linear (Seigneur et al., 1984, Seigneur et al., 1985, Saxena and Seigneur, 1986). It is therefore, of particular interest to investigate the sensitivity of the cloud concentrations of major chemical species, i.e., sulfate, nitrate, ammonium and hydrogen ions, to the levels of precursors. The precursors considered in this analysis were SO_2, NO_x, RHC and NH_3. The base case concentrations of SO_2 were very low (i.e., below or equal to the detection limit of 1 ppb) and, for the sensitivity study, we varied the SO_2 initial concentrations from 0 to 4 ppb. For the other sensitivity studies, the initial concentrations of NO_x, RHC and NH_3 were individually divided by a factor of two.

The sulfate cloud concentration and the sulfate wet deposition after two hours of simulation are presented in Figure 9-1 as function of the initial SO_2 concentration. These two curves show that the SO_2/sulfate relationship is non-linear. The response of sulfate concentration or wet deposition to the initial SO_2 concentration decreases as the initial SO_2 concentration increases. This result is due to the fact that the SO_2/sulfate system is oxidant limited at high SO_2 concentrations. In these simulations, the aqueous oxidation of SO_2 by H_2O_2 accounts for about 90 percent of the total sulfate formation whereas the aqueous oxidation of SO_2 by O_2 accounts for about 10 percent. The behavior of the SO_2/sulfate system characterized here is consistent with the results of previous studies (Seigneur et al., 1984, 1985).

The results of the other three sensitivity simulations are presented in Table 9-2.

The change in the NO_x initial concentrations affects solely the nitrate and hydrogen ion concentrations. The amount of nitrate present in the cloud, which was formed during the two-hour simulation, has been reduced from 1.24 ppb to 0.58 ppb. The aqueous

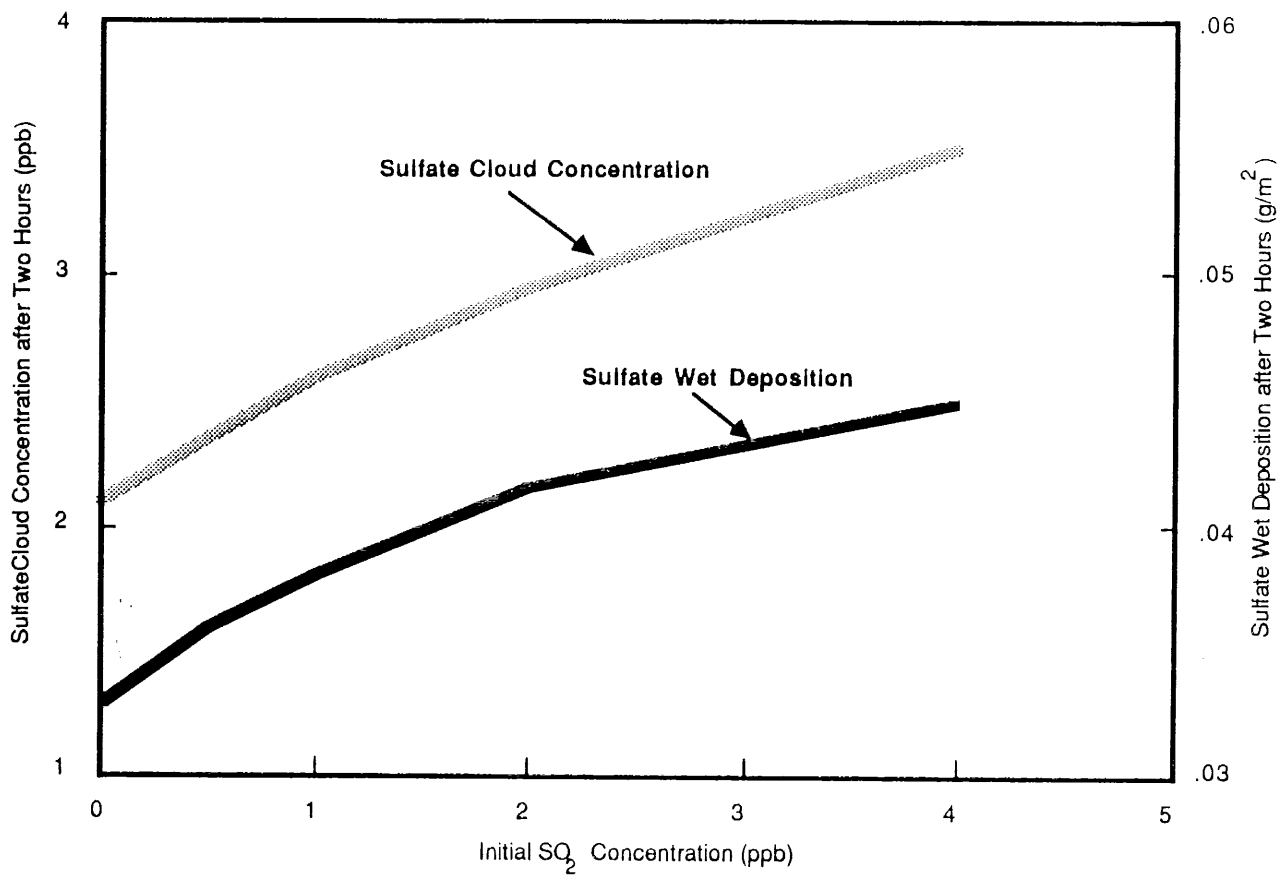

Figure 9-1 Sulfate Cloud Concentration and Wet Deposition after Two Hours as Function of the Initial SO_2 Concentration

19258/1/g/Air Poll./M31 6/14/88 pc/vk rev.1

Table 9-2. Major Species Concentrations after Two Hours for Various Precursor Levels

Change in Initial Concentration of Precursors	Sulfate (ppb)	Nitrate (ppb)	Ammonium (ppb)	pH
Base Case	2.53	7.00	7.06	3.73
NO_x concentrations divided by 2	2.53	6.39	7.06	3.78
RHC concentrations divided by 2	2.53	7.00	7.06	3.73
NH_3 concentrations divided by 2	2.53	7.00	3.46	3.47

reduction of NO_3 radicals is the dominant pathway (74% versus 61% in the base case) and the heterogeneous hydrolysis of N_2O_5 accounts for the rest of nitrate formation (26% versus 39% in the base case). As expected, the NO_3 aqueous reduction becomes a relatively more important pathway as the NO_x concentration decreases (see Section 7). The response of nitrate formation to a reduction in NO_x is nearly linear with a reduction of 53% in nitrate formation for a reduction of 50% in NO_x initial concentrations.

The reduction in RHC initial concentrations has no effect on sulfate and nitrate concentrations. This results is not too surprising since this sensitivity study addresses a nighttime simulation where no, or little, oxidant formation takes place. Therefore, the oxidation of SO_2 and NO_2 takes place through reaction with oxidants which were formed during daytime and are present at the beginning of the simulation. Reactive hydrocarbons, however, would have some effect on the oxidant levels produced during daytime. Three-dimensional simulations of oxidant and acid species formation need to be carried out to address this problem. It should be noted also that NO_x emission reductions would also affect oxidant levels and, consequently, affect nitrate formation in this manner. The effect of NO_x levels on oxidant levels does not appear in our two-hour nocturnal simulation but should be kept in mind when designing emission control strategies.

A reduction in NH_3 initial concentrations has a direct effect on NH_4^+ concentrations which are reduced proportionally. As a result, the pH decreases slightly since the cloud droplets become more acidic as NH_4^+ concentrations decrease.

SENSITIVITY TO PHYSICO-CHEMICAL PARAMETERS

There are some uncertainties associated with some key parameters of the cloud model and it is of particular interest to assess the sensitivity of the model output to these uncertainties. The parameters that were investigated here included the following:

(1) The rate of N_2O_5 heterogeneous hydrolysis
(2) The rate of NO_3 gas/droplet mass transfer
(3) The updraft velocity
(4) The liquid water content

The heterogeneous hydrolysis of N_2O_5 and the aqueous reduction of NO_3 are the two dominant pathways for the rate of formation of nitrate under the simulation conditions considered (see Sections 7 and 8).

Therefore, the first two parameters are critical to the accuracy of the model for nitrate concentration predictions.

The chemistry of the cloud is likely to be affected by two major parameters: the amount of liquid water available for aqueous chemistry and the rate of entrainment of chemical species into the cloud. The last two parametric sensitivity studies address these two questions.

The results of the sensitivity of the model predictions of nitrate and hydrogen ion concentrations to the N_2O_5 and NO_3 kinetic parameters are presented in Table 9-3.

In the base case, the N_2O_5 heterogeneous hydrolysis was calculated according to the kinetics reported by Harker and Strauss (1981). In the first sensitivity study, it was assumed that the heterogeneous hydrolysis of N_2O_5 would take place every time

Table 9-3. Nitrate and Hydrogen Ion Concentrations after Two Hours for Various Nitrate Formation Kinetics

Change in Kinetic Parameters	Nitrate (ppb)	pH
Base Case	7.00	3.73
N_2O_5 heterogeneous hydrolysis limited only by N_2O_5 diffusion	7.41	3.68
NO_3 accommodation coefficient equal to 1	7.00	3.73
NO_3 accommodation coefficient equal to 0.01	7.00	3.73
NO_3 accommodation coefficient equal to 10^{-6}	7.34	3.67

that a molecule of N_2O_5 would hit a water droplet. Therefore, the kinetics of N_2O_5 hetrogeneous hydrolysis is limited by the gas-phase diffusion of N_2O_5 and should be an upper limit to the actual rate. It appears that the amount of nitrate formed increases by 0.4 ppb which corresponds to a 30% increase from the base case. The N_2O_5 hydrolysis pathway accounts for 81% of nitrate formation (versus 39% in the base case) whereas the NO_3 aqueous oxidation pathway accounts for only 19% (versus 61% in the base case).

The formation of nitrate from the aqueous reduction of NO_3 radicals depends, in part, on the rate of mass transfer of NO_3 radicals from the gas phase to the aqueous phase. There is presently some uncertainty regarding the accommodation coefficient of NO_3 radicals on water droplets. In the base case, this accommodation coefficient has a value of 0.2 based on the data reported for HO_2 by Mozurkewich et al. (1987). We investigated the sensitivity of nitrate formation to the value of the NO_3 accommodation coefficient. This parameter was varied from 10^{-6} to 1. The results of three sensitivity simulations are reported in Table 9-3. It is interesting to note that as the accommodation coefficient of NO_3 decreases, the amount of nitrate formed increases. As NO_3 radicals are not scavenged by droplets, they react with NO_2 to form N_2O_5. Hydrolysis of N_2O_5 leads to two nitrate ions whereas aqueous reduction of NO_3 leads to only one nitrate ion. Therefore, more nitrate is found when the gas-phase conversion of NO_3 to N_2O_5 dominates the gas/droplet mass transfer of NO_3 radicals.

The sensitivity of the cloud chemistry calculations to two cloud physics parameters, the updraft velocity and the cloud water content, was investigated. The results of these two sensitivity studies are reported in Table 9-4 for the sulfate, nitrate, ammonium and hydrogen ion concentrations.

Table 9-4. Major Species Concentrations after Two Hours for Various Values of Cloud Physics Parameters

Change in Parameters	Sulfate (ppb)	Nitrate (ppb)	Ammonium (ppb)	pH
Base Case	2.53	7.00	7.06	3.73
Updraft Velocity multiplied by 2	1.76	4.36	5.51	4.00
Cloud Water Content multiplied by 2	2.60	7.02	7.06	4.01

An increase in the updraft velocity by a factor of two leads to a larger contribution of species entrained from below the cloud to the total cloud chemical composition. Since below-cloud initial concentrations are less than in-cloud initial concentrations, the cloud species concentrations are lower after two hours of simulation when the updraft velocity is higher. The pH increases from 3.73 to 4.00 as the acid species concentrations decrease.

The increase in cloud water content has no effect on chemically inert species such as ammonium ions. The concentrations (expressed in ppb) of sulfate and nitrate ions have increased slightly because of the larger volume of water available for chemical reactions. For example, reactions of SO_2 with O_2 and OH increase by factors of about 2 when the cloud water content increases by a factor of 2. The total amount of sulfate formed increases from 0.42 ppb to 0.50 ppb. It should be noted that the oxidation of SO_2 by H_2O_2 is not affected by the liquid water content because it is a fast reaction which is limited by the initial amount of either SO_2 or H_2O_2. The relative contribution of the major pathways to sulfate formation were 68% for the H_2O_2 aqueous reaction (versus 83% in the base case), 21% for the O_2 aqueous reaction (versus 12% in the base case), 10% for the OH aqueous reaction (versus 5% in the base case) and 1% for minor pathways.

The nitrate formation increases from 1.24 ppb to 1.26 ppb as the cloud water content increases. There is a slight increase in the NO_3 aqueous reduction pathway due to the larger amount of water since this pathway accounts for 66% of nitrate formation versus 61% in the base case. Because of the parallel decrease in NO_3 gas-phase radical concentration, the N_2O_5 pathway decreases slightly, thereby, compensating the increase in the NO_3 pathway.

SENSITIVITY TO ENVIRONMENTAL CONDITIONS

The base case simulation of 26 May 1985 pertains to the nighttime chemistry and transport of stratus clouds. It is of interest to study the variations in the chemical reactions that would occur as the environmental conditions change. Five different cases were considered.

(1) Daytime conditions
(2) Nighttime non-raining cloud
(3) Nighttime cloud free conditions (i.e., gas-phase chemistry only)
(4) Nighttime ground-level fog conditions
(5) Nighttime plume dispersed in a stratus cloud

The results of these simulations are summarized in Table 9-5 for sulfate, nitrate, ammonium and hydrogen concentrations.

The daytime simulation shows a slight increase in sulfate concentrations (0.17 ppb) which is due to an increase in the aqueous oxidation of SO_2 by OH(aq) and other minor SO_2 oxidation pathways. The increase in nitrate concentrations is more significant since it amounts to 0.62 ppb, i.e. about 9%. There is also a significant change in the major chemical pathways leading to nitrate formation. During daytime, high concentrations of OH radicals lead to a predominance of the gas-phase reaction of NO_2 with OH radicals (86% of nitrate formation versus a negligible amount at nighttime). The NO_3 aqueous reduction pathway decreased from 61% (nighttime) to 10% (daytime). The N_2O_5 hydrolysis pathway also decreased from 39% (nighttime) to 4% (daytime). These decreases in the relative importance of the NO_3 and N_2O_5 pathways result from the fact that NO_3 photolysis and reaction with NO lead to lower NO_3 concentrations during daytime than at night. During daytime, concentrations of phenoxy compounds increase (0.3 ppb in the cloud after two hours) and the reaction of NO_3 radicals with phenoxy compounds is a small but non-negligible pathway

Table 9-5. Major Species Concentrations after Two Hours for Various Environmental Conditions

Environmental Conditions	Sulfate (ppb)	Nitrate (ppb)	Ammonium (ppb)	pH
Base Case	2.53	7.00	7.06	3.73
Daytime Cloud	2.70	7.62	7.02	3.70
Nighttime Non-raining Cloud	3.80	9.70	10.6	3.59
Nighttime Cloud Free Conditions	3.15	8.60	10.6	--
Nighttime Fog	4.9	16.1	8.7	3.2
Nighttime Plume in Cloud	10.1	15.8	8.7	3.0

for nitrate formation (4% of the total nitrate formed). Because of higher concentration of sulfate and nitrate, the pH of the cloud droplets is slightly lower at the end of the daytime simulation than at the end of the nighttime simulation.

The non-raining cloud simulation differs from the base case only by the lack of precipitation. As a result, concentrations of soluble species are higher in the cloud since rain does not deplete these concentrations. The sulfate, nitrate and ammonium concentrations are higher by 50, 40 and 50 percent, respectively. The difference in nitrate concentration is less because nitrate is formed toward the end of the simulation and is not depleted by rainout as much as other species that are depleted throughout the two-hour simulation. The pH at the end of the non-raining cloud simulation is lower because of the presence of higher concentrations of sulfate and nitrate.

The nighttime cloud free simulation is best compared to the nighttime non-raining cloud simulations since there are no removal processes in both simulations. (The base case simulation involves rainout of soluble species which makes the comparison more difficult.) It appears that no sulfate formation takes place in the nighttime cloud free simulations. This result is consistent with the previous results that showed that the dominant pathways for sulfate formation in the nighttime simulation were aqueous reactions. Little nitrate formation takes place (0.24 ppb over the two-hour simulation); the N_2O_5 hydrolysis reaction is the dominant pathway.

In the nighttime fog simulation, all species initial concentrations were identical to those of the fourth layer of the base case cloud simulation (i.e., the layer corresponding to the aircraft measurements) except for NO, NO_2, and O_3 initial concentrations which were 40, 10 and 20 ppb, based on ground-level data (ARB,

1987). PAN concentrations were assumed to be 5 ppb. The results after two hours of simulation show high sulfate, nitrate and ammonium concentrations because there is no entrainment of lower concentrations and no rainout of soluble species. The amount of sulfate and nitrate formed are 0.9 and 0.3 ppb, respectively. Sulfate formation is limited by the initial amount of SO_2 present. It takes place primarily through aqueous reaction of SO_2 with H_2O_2 (90%). For nitrate formation, the gas-phase reaction of NO_2 with OH radicals is the dominant, yet limited, pathway. Concentrations of OH radicals are not negligible in fog, about $3x10^{-6}$ ppb, because of the reaction of PAN in presence of NO (Seigneur and Saxena, 1984). Concentrations of NO_3 radicals, on the other hand, are small because NO emissions at ground level deplete O_3 rapidly at night and the reaction of NO_2 with O_3, therefore, does not take place to produce NO_3.

The plume simulation was conducted by assuming that the initial NO_x and SO_2 concentrations were 100 ppb each. The NO_x concentration consisted of 90 ppb of NO and 10 ppb of NO_2. These concentrations are consistent with measurements reported by Richards et al. (1983a) in the vicinity of the Fontana area in 1981-1982. About 11 ppb of sulfate are formed during the two-hour plume simulation. The aqueous oxidation of SO_2 by O_2 accounts for 90% of sulfate formation whereas the remaining 10% result from the oxidation of SO_2 by H_2O_2. A negligible amount of nitrate was formed. Concentrations of NO_3 were small because, in the simulation, all O_3 was depleted by NO and no NO_3 was, therefore, formed. Formation of OH radicals at night can result from reaction of NO with PAN and NO_3 with aldehydes or phenoxy compounds. NO_3 concentrations are low in a NO plume and PAN concentrations were below the detection limit of 1 ppb. Therefore, no major pathway was available for nitrate formation.

It is particularly interesting to note that in a plume, HMSA formation takes place rapidly. After one hour, the HMSA

concentration is equal to $1x10^{-6}$ M, which is commensurate with values observed in clouds (Richards et al., 1983b). As diffusion takes place, the HMSA concentration decreases to $0.02x10^{-6}$ M. This value of HMSA concentration is higher than the value expected from equilibrium between SO_2 and HCHO because the HMSA dissociation reaction is slower than the formation reaction. This simulation confirms that S(IV) concentrations that were observed in 1981-1982 could be explained as being HMSA resulting from the reaction of SO_2 with HCHO in cloudwater in plumes.

Section 10
CLOUD CHEMISTRY OF ORGANIC ACIDS

INTRODUCTION

The theoretical investigation of acid formation in clouds and fog in the Los Angeles basin has focused so far on the formation of inorganic acids such as sulfuric acid (H_2SO_4) and nitric acid (HNO_3) (Jacob and Hoffmann, 1983, Seigneur and Saxena, 1984, Seigneur et al., 1985). Recent measurements of rainwater in the Los Angeles basin have suggested that organic acids may also contribute significantly to the acidity of cloud, fog and rainwater (Grosjean, 1988, Kawamura et al., 1985). Therefore, it is desirable to include a chemical mechanism for organic acid formation in a mathematical model of atmospheric acid formation. This section presents the development of a chemical kinetic mechanism for organic acids and the results of some model simulations.

CHEMICAL KINETIC MECHANISM

The two major organic acids which have been identified in the Los Angeles basin are formic acid (HCOOH) and acetic acid (CH_3COOH) (Kawamura et al., 1985, Grosjean, 1988). Therefore, the chemical kinetic mechanism for organic acids consists of the reactions that directly affect the concentrations of these two acids in the gas phase and the liquid phase.

The chemical kinetic mechanism of Seigneur and Saxena (1988) is used for sulfuric and nitric acid formation. The chemical kinetic mechanism for organic acid formation is presented in Table 10-1. It may be noted that some reactions presented in Table 10-1 were already included in the mechanism of Seigneur and Saxena (1988) (e.g., formaldehyde chemistry, peroxyacetic acid reactions). This chemical kinetic mechanism may be summarized as follows.

Table 10-1: Chemical Kinetic Mechanism for Organic Acids

Reaction	Equilibrium or Rate Constant at 298 K	Enthalpy or Activation Energy	Reference
Gas-Phase Kinetics			
$HCHO+HO_2(+NO) \rightarrow HCOOH+HO_2+NO_2$	$14.8\ ppm^{-1}\ min^{-1}$		Lurmann et al. (1986)
$CH_2O_2+H_2O \rightarrow HCOOH$	$5.92 \times 10^{-3}\ ppm^{-1}\ min^{-1}$	Lurmann et al. (1986)	
$CH_3CHO_2+H_2O \rightarrow CH_3COOH$	$5.92 \times 10^{-3}\ ppm^{-1}\ min^{-1}$		Lurmann et al. (1986)
$HCOOH+OH \rightarrow HO_2+CO_2+H_2O$	$474\ ppm^{-1}\ min^{-1}$		Zetzsch and Stuhl (1982)
$CH_3COO_2+HO_2 \rightarrow CH_3COO_2H+O_2$	$9600\ ppm^{-1}\ min^{-1}$		Whitten and Gery (1986)
Gas-Phase/Aqueous-Phase Equilibria			
$HCHO\ (g) \rightleftarrows HCHO\ (aq)$	$3.5\ M\ atm^{-1}$		Hoffmann and Calvert (1985)
$CH_3CHO\ (g) \rightleftarrows CH_3CHO\ (aq)$	$13\ M\ atm^{-1}$	$-11\ kcal\ mol^{-1}$	Snider and Dawson (1985)
$HCOOH\ (g) \rightleftarrows HCOOH\ (aq)$	$3.7 \times 10^{3}\ M\ atm^{-1}$	$-11.4\ kcal\ mol^{-1}$	Latimer (1952)
$CH_3COOH\ (g) \rightleftarrows CH_3COOH\ (aq)$	$8.8 \times 10^{3}\ M\ atm^{-1}$	$-12.8\ kcal\ mol^{-1}$	CRC (1986)
$CH_3COO_2H\ (g) \rightleftarrows CH_3COO_2H\ (aq)$	$4.4 \times 10^{2}\ M\ atm^{-1}$	$-12.3\ kcal\ mol^{-1}$	Lind and Kok (1986)
Aqueous-Phase Equilibria			
$HCHO\ (aq) \rightleftarrows H_2C(OH)_2\ (aq)$	1.8×10^{3}	$-12.9\ kcal\ mol^{-1}$	Ledbury and Blair (1925)
$CH_3CHO\ (aq) \rightleftarrows CH_3CH(OH)_2\ (aq)$	1.2	$-5\ kcal\ mol^{-1}$	Bell (1966)
$HCOOH\ (aq) \rightleftarrows HCOO^- + H^+$	$1.78 \times 10^{-4}\ M$	$-0.3\ kcal\ mol^{-1}$	Sillen and Martell (1964)
$CH_3COOH\ (aq) \rightleftarrows CH_3COO^- + H^+$	$1.7 \times 10^{-5}\ M$	$-0.1\ kcal\ mol^{-1}$	Sillen and Martell (1964)

Table 10-1: Chemical Kinetic Mechanism for Organic Acids (Continued)

Reaction	Equilibrium or Rate Constant at 298 K	Enthalpy or Activation Energy	Reference
Aqueous-Phase Kinetics			
$H_2C(OH)_2(aq)+OH(aq) \rightarrow HCOOH(aq)+HO_2(aq)+H_2O(l)$	$1.2 \times 10^{11}\ M^{-1}\ min^{-1}$	$3.0\ kcal\ mol^{-1}$	Bothe and Schulte - Frohlinde (1980), Anbar and Neta (1967)
$H_2C(OH)_2(aq)+O_3(aq) \rightarrow Products$	$6.0\ M^{-1}\ min^{-1}$		Hoigne and Bader (1983)
$HCOOH(aq)+OH(aq) \rightarrow CO_2(aq)+HO_2(aq)+H_2O(l)$	$1.2 \times 10^{10}\ M^{-1}\ min^{-1}$	$3.0\ kcal\ mol^{-1}$	Anbar and Neta (1967)
$HCOO^-+OH(aq) \rightarrow CO_2(aq)+HO_2(aq)+OH^-$	$1.5 \times 10^{11}\ M^{-1}\ min^{-1}$	$3.0\ kcal\ mol^{-1}$	Anbar and Neta (1967)
$CH_3CHO(aq)+OH(aq)(+\ HO_2(aq)) \rightarrow CH_3COO_2H(aq)$	$3.0 \times 10^{10}\ M^{-1}\ min^{-1}$	$3.0\ kcal\ mol^{-1}$	Merz and Water (1949)
$CH_3COO_2(g)\ (+\ HO_2(aq)) \rightarrow CH_3COO_2H(aq)$	Diffusion limited		This work
$CH_3COO_2H(aq)\ (+\ H_2O(l)) \rightarrow CH_3COOH(aq)+H_2O_2(aq)$	$3.0 \times 10^{-4}\ min^{-1}$		Koubeck and Edwards (1963)
$CH_3COO_2H(aq)+OH(aq) \rightarrow Products$	$1.2 \times 10^{9}\ M^{-1}\ min^{-1}$	$3.7\ kcal\ mol^{-1}$	Jacob and Wofsy (1986)
$CH_3COO_2H(aq)+HSO_3^- \rightarrow CH_3COOH(aq)+SO_4^{2-} + H^+$	$(3.02 \times 10^{9}[H^+] + 3.6 \times 10^{4})M^{-1}\ min^{-1}$	$8.0\ kcal\ mol^{-1}$	Hoffmann and Calvert (1985)
$CH_3CH(OH)_2(aq)+OH(aq) \rightarrow CH_3COOH(aq)+HO_2(aq)+H_2O(l)$	$3.0 \times 10^{10}\ M^{-1}\ min^{-1}$	$3.0\ kcal\ mol^{-1}$	Merz and Water (1949)
$CH_3COOH(aq)+OH(aq) \rightarrow Products$	$1.2 \times 10^{9}\ M^{-1}\ min^{-1}$	$3.7\ kcal\ mol^{-1}$	Fahrataziz and Ross (1977)
$CH_3COO^-+OH(aq) \rightarrow Products$	$4.2 \times 10^{9}\ M^{-1}\ min^{-1}$	$3.0\ kcal\ mol^{-1}$	Fahrataziz and Ross (1977)

Formic acid is formed through two reactions in the gas phase (oxidation of formaldehyde by HO_2 and hydrolysis of the Criegee radical CH_2O_2) and through one reaction in the aqueous phase (oxidation of hydrated formaldehyde by OH). It is consumed through reaction with OH in both the gas phase and the aqueous phase.

Acetic acid is formed through hydrolysis of the Criegee radical CH_3CHO_2 in the gas phase, reaction of acetaldehyde with OH radicals, hydrolysis of peroxyacetic acid (CH_3COO_2H) and reaction of peroxyacetic acid with bisulfite ions (HSO_3^-) in the aqueous phase.

The formation of peroxyacetic acid occurs in the gas phase via reaction of peroxyacetyl radicals (CH_3COO_2) with HO_2 radicals and, in the aqueous phase, via dissolution of CH_3COO_2 radicals and subsequent reaction with HO_2 radicals and via reaction of acetaldehyde with OH radicals. Peroxyacetic acid is consumed in the aqueous phase via hydrolysis, reaction with OH radicals and reaction with HSO_3^-.

The chemical kinetic mechanism for organic acid formation consists of five gas-phase reactions, five gas-phase/aqueous-phase equilibria, four aqueous-phase equilibria and twelve aqueous-phase reactions.

MODEL SIMULATION

A model simulation was conducted using the first hour of the base case nighttime simulation of 26 May 1985 without rainout.

Little amount of organic acids was formed during this one-hour simulation since only 0.16 ppb of formic acid and 0.0045 ppb of acetic acid were formed. The corresponding aqueous-phase

concentrations were 0.06 ppb (1.8×10^{-6} M) for formic acid and 0.002 ppb (7×10^{-8} M) for acetic acid. Since these two organic species are weak acids, only a fraction of these concentrations is present in the ionic form. The concentration of $HCOO^-$ was 8.2×10^{-7}M (i.e., 45% of the total aqueous-phase concentration) and the concentration of CH_3COO^- was 5×10^{-9} (i.e., 7% of the total aqueous-phase concentration). These low concentrations of organic acidic species have negligible effect on the cloud pH.

It should be noted that the simulation considered here is a one-hour nighttime simulation. Most chemical processes leading to organic acid formation involve OH and HO_2 radicals which are typically present in minute concentrations at night but are significant during the day. Therefore, organic acid formation should be significantly more important during daytime than during this nighttime simulation. Further work should be carried out to investigate the chemistry of organic acid formation under a variety of conditions (e.g., daytime, clouds, gas-phase, etc.).

REFERENCES

Anbar, M. and P. Neta (1967) A compilation of specific bimolecular rate constants for reactions of hydrated electrons, hydrogen atoms and hydroxyl radicals with inorganic and organic compounds in aqueous solution. Int. J. Appl. Radiat. Isot., Vol. 18, pp. 493-523.

ARB (1987) Air Quality Report, California Air Resources Board, Sacramento, California.

Bell, R. P. (1966) The reversible hydration of carbonyl compounds. Adv. Phys. Org. Chem., Vol. 4, pp. 1-29.

Betterton, E. A. and M. R. Hoffmann (1988) Henry's law constants of some environmentally important aldehydes, Environ. Sci. Technol., Vol. 22, pp. 1415-1418.

Bothe, E. and D. Schulte - Frohlinde (1980) Reaction of dihydroxymethyl radical with molecular oxygen in aqueous solution Z. Naturforsch. B., Anorg. Chem. Org. Chem., Vol. 35, pp. 1035-1039.

CRC (1986) Handbook of Chemistry and Physics, 66th ed., R. C. Weast, ed., Chemical Rubber Company, Cleveland, Ohio.

Fahrataziz, and A. B. Ross (1977) Selected specific rates of reactions of transients from water in aqueous solution. III. Hydroxyl radical and perhydroxyl radical and their radical ions. NSRDS-NBS., U.S. Dept. of Commerce, Washington, D.C.

Gautier, O., R. W. Carr and C. Seigneur (1985) Variational sensitivity analysis of a photochemical smog mechanism. Int. J. Chem. Kinet., Vol. 17, pp. 1347-1369.

Grosjean, D. (1988) Aldehydes, carboxylic acids and inorganic nitrate during NSMCS. Atmos. Environ., in press.

Harker, A.B. and D. R. Strauss (1981) Kinetics of the heterogeneous hydrolysis of dinitrogen pentoxide over the temperature range 214-263 K, Rockwell International Science Center, Federal Aviation Administration Publication FAA-EE-81-3.

Hoffmann, M. R. and J. G. Calvert (1985) Chemical transformation modules for Eulerian acid deposition models, Vol. II, The aqueous phase chemistry, National Center for Atmospheric Research, Boulder, Colorado.

Hoigne, J. and H. Bader (1983) Rate constants of reactions of ozone with organic and inorganic compounds in water, 1, Non-dissociating organic compounds. Water Res., Vol. 17, pp. 173-183.

Huie, R. E. and P. Neta (1987) Rate constants for some oxidations of S(IV) by radicals in aqueous solutions. Atmos. Environ., Vol. 21, pp. 1743-1747.

Ibusuki, T. and K. Takeuchi (1987) Sulfur dioxide oxidation by oxygen catalyzed by mixtures of manganese (II) and iron (III) in aqueous solution at environmental reaction conditions. Atmos. Environ., Vol. 21, pp. 1555-1560.

Jacob, D. J., and M. R. Hoffmann (1983) A dynamic model for the production of H^+, NO_3, and SO_4 in urban fog. J. Geophys. Res., Vol. 88, pp. 6611-6621.

Jacob, D. J. and S. C. Wofsy (1988) Photochemical production of carboxylic acids in a remote continental atmosphere, in Acid Deposition Processes at High Elevation Sites, M. H. Unsworth, ed., Reidel, Dordrecht, The Netherlands, in press.

John, W., S.M. Wall, and J. L. Ondo (1985) Dry acid deposition on materials and vegetation: Concentrations in ambient air, Report to California Air Resources Board, Sacramento, California.

Kawamura, K., L. L. Ng and I. R. Kaplan (1985) Determination of organic acids (C_1 - C_{10}) in the atmosphere, motor exhaust, and engine oils. Environ. Sci. Technol., Vol. 19, pp. 1082-1086.

Kessler, E. (1969) On the distribution and continuity of water substance in atmospheric circulations. Meterol. Monographs, Vol. 10, 85 pp.

Killus, J. P. and G. Z. Whitten (1985) Behavior of trace NO_x species in the nighttime urban atmosphere, J. Geophys. Res., Vol. 90, pp. 2430-2432.

Koenig, L. R. and F. W. Murray (1976) Ice-bearing cummulus cloud evolution: Numerical simulation and general comparison against observation. J. Appl. Meterol.. Vol. 15, pp. 747-762.

Koubeck, E. and J. D. Edwards (1963) The aqueous photochemistry of peroxychloroacetic acid. Inorg. Chem., Vol. 28, pp. 2157-2160.

Latimer, W.M. (1952) The Oxidation States of the Elements and their Potentials in Aqueous Solutions, 2nd ed., Prentice Hall, New York.

Ledbury, W. and E. W. Blair (1925) The partial formaldehyde vapour pressure of aqueous solution of formaldehyde, II. J. Chem. Soc., Vol. 127, pp. 2832-2839.

Lind, J.A. and G.L. Kok (1986) Henry's law determinations for aqueous solutions of hydrogen peroxide, methylhydroperoxide, and peroxyacetic acid. J. Geophys. Res., Vol. 91, pp. 7889-7895.

Lurmann, F. W., A.C. Lloyd, and R. Atkinson (1986) A chemical mechanism for use in long-range transport/acid deposition computer modeling. J. Geophys. Res., Vol. 91, pp. 10905-10936.

Martin, L. R. (1984) Kinetic studies of sulfite oxidation in aqueous solution. In SO_2, NO and NO_2 Oxidation Mechanisms (edited by Calvert, J. G.), pp. 63-100, Butterworth, Boston, Massachusetts.

Martin, L.R. and M.W. Hill (1987) The iron-catalyzed oxidation of sulfur: Reconciliation of the literature rates. Atmos. Environ., Vol. 21, pp. 1487-1490.

Martin, L. R. and M. W. Hill (1988) The manganese catalyzed oxidation of sulfur: Ionic strength and the literature rates. Atmos. Environ., in press.

Merz, J. H. and W. A. Waters (1949) Some oxidations involving the free hydroxyl radical. J. Chem. Soc., pp. S15-S25.

Mozurkewich, M., P.H. McMurry, A. Gupta and J. G. Calvert (1987) Mass accommodation coefficient for HO_2 radicals on aqueous particles, J. Geophys. Res., Vol. 92, pp. 4163-4170.

Pilinis, C. and J. H. Seinfeld (1987) Continued development of a general equilibrium model for inorganic multicomponent atmospheric aerosols. Atmos. Environ., Vol. 21, pp. 2453-2466.

Richards, L.W. (1983) Comments on the oxidation of NO_2 to nitrate - day and night. Atmos. Environ., Vol. 17, pp. 397-402.

Richards, L. W., J. A. Anderson, D. L. Blumenthal, S. L. Duckhorn, and J. A. McDonald (1983a) "Characterization of reactants, reaction mechanisms, and reaction products leading to existence of acid rain and acid aerosol conditions in southern California". Report to California Air Resources Board, Sacramento, California.

Richards, L. W., J. A. Anderson, D. J. Blumenthal, J. A. McDonald, G. L. Kok, and A. L. Lazrus (1983b) Hydrogen peroxide and sulfur (IV) in Los Angeles cloud water. Atmos. Environ., Vol. 17, pp.911-914.

Richards, L. W., J. A. Anderson, D. L. Blumenthal and J. A. McDonald (1985) "Characterization of the composition and three-dimensional distribution of acidity in southern California clouds." Report to California Air Resources Board, Sacramento, California.

Richards, L. W., J. A. Anderson, N. L. Alexander, D. L. Blumenthal, W. R. Knuth and J. A. McDonald (1987) "Characterization of reactants, mechanisms, and species in south coast air basin cloudwater." Report to California Air Resources Board, Sacramento, California.

Richards, L. W. (1988) private communication, Sonoma Technology, Inc., Santa Rosa, California

Russell, A. G. and G. R. Cass (1984) Acquisition of regional air quality model validation data for nitrate, sulfate, ammonium ion and their precursors. Atmos. Environ., Vol. 18, pp. 1815-1827.

Saxena, P. and C. Seigneur (1986) The extent of nonlinearity in the atmospheric chemistry of sulfate formation. J. Air Pollut. Control Assoc., Vol. 36, pp. 1151-1154.

Seigneur, C., and P. Saxena (1984) A study of atmospheric acid formation in different environments. Atmos. Environ., Vol. 18, pp. 2109-2124.

Seigneur, C., P. Saxena, and P. M. Roth (1984) Computer simulations of the atmospheric chemistry of sulfate and nitrate formation. Science, Vol. 225, pp. 1028-1030.

Seigneur, C. and P. Saxena (1985) The impact of cloud chemistry on photochemical oxidant formation. Wat. Air Soil Pollut., Vol. 24, pp. 419-429.

Seigneur, C., P. Saxena, and V. A. Mirabella (1985) Diffusion and reaction of pollutants in stratus clouds -- Application to nocturnal acid formation in plumes. Environ. Sci. Technol., Vol. 19, pp. 821-828.

Seigneur. C. and H. M. Barnes (1986) Technical considerations in regional aerosol modeling in Air Pollution Modeling and Its Application, Vol. 5, pp. 343-369, C. de Wispelaere, ed., Plenum Press, New York, New York.

Seigneur, C. (1987) Computer simulation of air pollution chemistry. Environ. Software, Vol. 2, pp. 116-127.

Seigneur, C. and P. Saxena (1988) A theoretical investigation of sulfate formation in clouds. Atmos. Environ., Vol. 22, pp. 101-115.

Sillen, G. L. and A. E. Martell (1964) Stability constants of metal-ion complexes. Spec. Publ. Chem. Soc. Vol. 17, p. 357.

Snider, J. R. and G. A. Dawson (1985) Tropospheric light alcohols, carbonyls, and acetonitrile: Concentrations in the southwestern United States and Henry's law data. J. Geophys. Res., Vol. 90, pp. 3797-3805.

Sverdrup, G., C. W. Spicer, and G. F. Ward (1987) Investigation of the gas phase reaction of dinitrogen pentoxide with water vapor. Int. J. Chem. Kinet., Vol. 19, pp. 191-205.

Whitten, G. Z. and M. W. Gery (1986) "Development of CBM-X Mechanisms for Urban and Regional AQSMs". EPA-600/3-86-012, U.S. Environmental Protection Agency, Research Triangle Park, North Carolina.

Wobus, H. B. et al. (1971) Calculation of the terminal velocity of water drops. J. Appl. Meteor., Vol. 10, pp. 751-754.

Zetzsch, C. and F. Stuhl (1982) Rate constants for reactions of OH with carbonic acids, in Proc. 2nd European Symp. Phys. - Chem. Behavior of Atmospheric Pollutants, pp. 129-137, D. Reidel, Hingham, Massachusetts.